JHR 99: 1–46 (2026)
doi: 10.3897/jhr.99.167713
https://jhr.pensoft.net

RESEARCH ARTICLE

JOURNAL OF Hymenoptera RESEARCH
A peer-reviewed open-access journal
The International Society of Hymenopterists

Review of the subgenus *Paropheltes* Cameron of genus *Netelia* Gray (Hymenoptera, Ichneumonidae, Tryphoninae) from Taiwan, with a proposal for improving male genitalia observations

Hsaun-Pu Chen[1,2], Kazuhiko Konishi[3,4], Shiuh-Feng Shiao[2]

1 *Laboratory of Systematic Entomology, Graduate School of Agriculture, Hokkaido University, Kita 9-jo Nishi 9-chome, Kita-ku, Sapporo, Hokkaido 060-0809, Japan* **2** *Department of Entomology, National Taiwan University, No. 1, Sec. 4, Roosevelt Rd., Da'an Dist., Taipei 106, Taiwan* **3** *Hokkaido University Museum, Kita 10-jo, Nishi 8-chome, Kita-ku, Sapporo, Hokkaido 060-0810, Japan* **4** *Entomological Laboratory, Faculty of Agriculture, Ehime University, Tarumi 3-5-7, Matsuyama, Ehime 790-8566, Japan*

Corresponding author: Shiuh-Feng Shiao (sfshiao@ntu.edu.tw)

Academic editor: Tamara Spasojevic | Received 4 August 2025 | Accepted 2 December 2025 | Published 8 January 2026

https://zoobank.org/17CC4420-A944-4C44-AB34-AD8DB365760F

Citation: Chen H-P, Konishi K, Shiao S-F (2026) Review of the subgenus *Paropheltes* Cameron of genus *Netelia* Gray (Hymenoptera, Ichneumonidae, Tryphoninae) from Taiwan, with a proposal for improving male genitalia observations. Journal of Hymenoptera Research 99: 1–46. https://doi.org/10.3897/jhr.99.167713

Abstract

An integrated taxonomic approach combining morphology and *COI* barcode is applied to the subgenus *Paropheltes* Cameron of the nocturnal Darwin wasp genus *Netelia* Gray from Taiwan. This subgenus is recorded from Taiwan for the first time based on four previously described species (*N.* (*Paro.*) *fulginosa* Konishi, 1996, *N.* (*Paro.*) *guptai* Kaur & Jonathan, 1979, *N.* (*Paro.*) *savchenkoi* Tolkanitz, 1981, and *N.* (*Paro.*) *yui* Konishi, 2000) and a new species (*N.* (*Paro.*) *dalupalringi* Chen, Konishi & Shiao, **sp. nov.**). The new species is distinguished from its congeners by a newly proposed key to the Taiwanese species and by male genitalia characters, including the rounded blunt apex of the gonostyle, semi-circular pad projected dorsobasally, parallel-sided brace narrowed apically, as well as the presence of a submarginal spine on the gonostyle. Improved methods for observation of male genitalia, particularly to enhance the visibility of the pad, a key membranous diagnostic feature, are proposed, and their implications are discussed. DNA-based species delimitation is conducted for three species with available DNA barcodes. Additionally, a *COI*-based phylogeny is reconstructed to assess the monophyly of this subgenus, confirming *Paropheltes* as a polyphyletic group.

Keywords

Darwin wasps, DNA barcode, integrative taxonomy, new species, new record

Copyright *Hsaun-Pu Chen et al.* This is an open access article distributed under the terms of the Creative Commons Attribution License (CC BY 4.0), which permits unrestricted use, distribution, and reproduction in any medium, provided the original author and source are credited.

Introduction

The genus *Netelia* Gray, 1860 represents one of the most diverse groups of nocturnal and crepuscular Darwin wasps (Hymenoptera: Ichneumonidae), comprising 331 valid species (Yu et al. 2016; Shimizu and Broad 2020; Pham et al. 2021; Konishi et al. 2022). Although most members of the subfamily Tryphoninae parasitize symphytans, the tribe Phytodietini (*Netelia* and *Phytodietus* Gravenhorst, 1829) is exceptional in targeting larval lepidopterans as koinobiont ectoparasitoids (Broad et al. 2018).

The high similarity in the general appearance of *Netelia* species has historically limited species-level diagnosis based on various morphological characters, leading to considerable taxonomic confusion. It was not until Townes (1939) discovered the highly specialized gonostyle of the male genitalia—characterized by autapomorphic traits, the "brace' and "pad" — as helpful characters for species-level identification, the taxonomic system for this genus was then established.

Following Townes' system, this genus has been subdivided into 12 subgenera by subsequent researchers based on genital and other characters (Townes 1939; Townes et al. 1961; Tolkanitz 1974; Kaur and Jonathan 1976; Konishi 1986b, 2010). By far, the majority of described species of *Netelia* are classified into the nominotypical subgenus (194 species according to Yu et al. 2016). Faunistic studies have been conducted in European (Delrio 1975), Nearctic region (Townes 1939), Russia (Tolkanitz 1974, 1981a, 1981b, 1999), Korea (Lee and Cha 1996; Choi and Lee 2017, 2019), Japan (Konishi 1985, 1986a, 1986b, 1991, 1992, 1996a, 1996b, 1996c, 2005, 2010, 2014), and the Oriental region (Kaur and Jonathan 1979; Pham et al. 2021; Konishi et al. 2022). However, the current species diversity of this genus could still be highly underestimated, as more than 50 undescribed species were found in Costa Rica (Gauld 1997) and about 100 undescribed species from the Afrotropical region were found in the Townes collection (Utah State University, Logan, Utah, USA) (Andrew Bennett personal communication).

Additionally, the male-based taxonomic system of *Netelia* raises problems such as the difficulties in identifying the females and misinterpretation of the male genital characters due to unstandardized techniques for male genitalia observation. Therefore, integrated taxonomic approaches (Dayrat 2005; Yeates et al. 2010), as well as a proposal for standardizing the morphological observations of the male genitalia, are necessary for systematic studies of this genus.

For the male genitalia observation, the "pad," a membranous structure whose shape serves as a key species-level diagnostic character, becomes translucent after maceration treatment and make its shape difficult to interpret due to the limitations of the microscope (Townes 1939), or when using observation techniques that employ a strong transmitted light source or lack staining. In fact, variations in observation methods among authors have led to potential misidentifications due to misinterpretation of pad outlines. For example, the genital illustrations

of *Netelia* (*Netelia*) *silantjewi* (Kokujev, 1899) in Kaur and Jonathan (1979) and Konishi (2005) show significant differences in the shape of the pad. In Kaur and Jonathan (1979: 229, fig. 34e), the pad appears open, with only a dorso-basal projection, whereas in Konishi (2005: 101, fig. 29F), it is depicted as crescent-shaped. It is possible that Kaur and Jonathan observed the pad using the transmitted light source of a microscope, which may have resulted in poor visibility and a misinterpretation of its outline. This case underscores the importance of proposing improved methods for genital observation in this genus.

The subgenus *Paropheltes* Cameron, 1907 comprises 46 described species, making it the second largest subgenus following the nominotypical subgenus *Netelia* (no other subgenus has more than 23 described species) (Yu et al. 2016). It is distributed worldwide, particularly in the Holarctic region (Bennett 2015; Yu et al. 2016). Reliable host records for this subgenus are limited to Geometridae (Brischke 1880; Morley 1915). This subgenus can be diagnosed by having a combination of characters involving the occipital carina, mesopleuron sculptures, scutellar lateral carina, fore wing venation, hind tarsal claw pectens, and the color pattern of the mesosoma (details specified in the Taxonomy section). However, the male genitalia of *Paropheltes* species exhibit high heterogeneity and thus difficult to use for defining the subgenus (Konishi 1996a). In addition, the boundary of this subgenus remains vague and may be confused with subgenera *Longiterebates* Kaur & Jonathan, 1976 and *Prosthodocis* Enderlein, 1912. Considering also the polyphyly revealed by morphological phylogeny (Coronado-Rivera 2009), further systematic study is necessary to clarify the phylogenetic relationship and redefine the subgeneric boundary.

Taiwan is a large continental island in East Asia characterized by mountainous terrain with an impressive elevation range from sea level up to 3,952 meters (Klose 2006). This elevation range creates various habitats, establishing Taiwan as a biodiversity hotspot and facilitating endemism (e.g., He et al. 2018). However, the Taiwanese fauna of the genus *Netelia* has not received comprehensive taxonomic attention since the pioneering studies by Uchida (1928, 1934). While a checklist (Chiu et al. 1984) and subsequent publications (Konishi 1986a, 1991, 1996c, 2000, 2005, 2010, 2012, 2014; Pham et al. 2021; Konishi et al. 2022) recorded 22 species across eight subgenera in Taiwan, recent findings from the first author's thesis (Chen 2024) suggest that the actual species richness of *Netelia* in Taiwan is underestimated and should likely be increased four-fold.

As the first installment of the systematics studies of Taiwanese *Netelia* (Chen 2024), this study reviews and reports the first record of the subgenus *Paropheltes* from Taiwan and introduces an improved technique for observing male genitalia characters. Illustrations and a diagnostic key for Taiwanese species, with emphasis on male genitalia, are provided. DNA-based species delimitation was conducted for available species, and a *COI*-based phylogeny of world *Netelia* sequences obtained from Barcode of Life Data Systems (BOLD) (Ratnasingham and Hebert 2007) were reconstructed to infer the monophyly of this subgenus.

Materials and methods

Specimen used

The freshly collected specimens used in this study were sampled by using a light trap. The depositions of the studied specimens were listed as follows:

NMNS: National Museum of Natural Science, Taichung, Taiwan; **TARI:** Taiwan Agricultural Research Institute, Taichung, Taiwan; **NARO:** Institute for Agro-Environmental Sciences, National Agriculture and Food Research Organization, Tsukuba, Ibaraki, Japan; **KPMNH:** Kanagawa Prefectural Museum of Natural History, Odawara, Kanagawa, Japan; **SEHU:** Laboratory of Systematic Entomology, Hokkaido University Museum, Sapporo, Hokkaido, Japan; **SIZU:** I. I. Schmalhausen Institute of Zoology, Kyiv, Ukraine.

An additional format for citing exact label data for the type specimens was used as follows: quotation marks (“ ”) cited the original texts on the label; and brackets ([ ]) provided the English translation, interpreted localities, and other comments on the original text.

Other comparative material for confirming identification is listed below:

Holotype of *Paniscus nigrus* (=*Netelia* (*Paropheltes*) *caucasica*). Japan • 1 ♀; “円山” [Hokkaido: Sapporo: Maruyama]; “6. 6” [6. VI. Unknown]; S. Matsumura leg.; Voucher: SEHU. Holotype of *Netelia* (*Paropheltes*) *ermolenkoi*. KURIL ISLANDS • 1 ♀; “Курилы, Шикотан, бухта Церковная” [Kuril Islands: Shikotan: Tserkovnaya Bay]; 25. VII. 1976; “Ермоленко” [Ermolenko] leg.; Voucher: SIZU.

Morphological terminologies and abbreviations

The terminologies of structures followed Broad et al. (2018) and male genitalia followed Dal Pos et al. (2023), and the measurements and indices mainly followed Gauld and Mitchell (1981) and Konishi (1985, 2005). Descriptions of the cuticular microsculpture as per Eady (1968). The morphological structures and the measurement methods were illustrated in Figs 1–3. Morphological abbreviations adapted for general description and their definitions are listed below:

Head in dorsal view (Fig. 1A):

OD: lateral ocellus diameter; **POL:** postero-ocellar line, minimum distance between lateral ocelli; **HL:** length of head; **HW:** width of head.

Head in lateral view (Fig. 1B):

BMW: basal mandibular width; **MSL:** length of malar space, the minimum distance between the eye and mandibular base measured in ventro-lateral view;

GOI: geno-orbital index, $\frac{\text{Maximum width of eye in lateral view}}{\text{Width of gena at the same line}}$

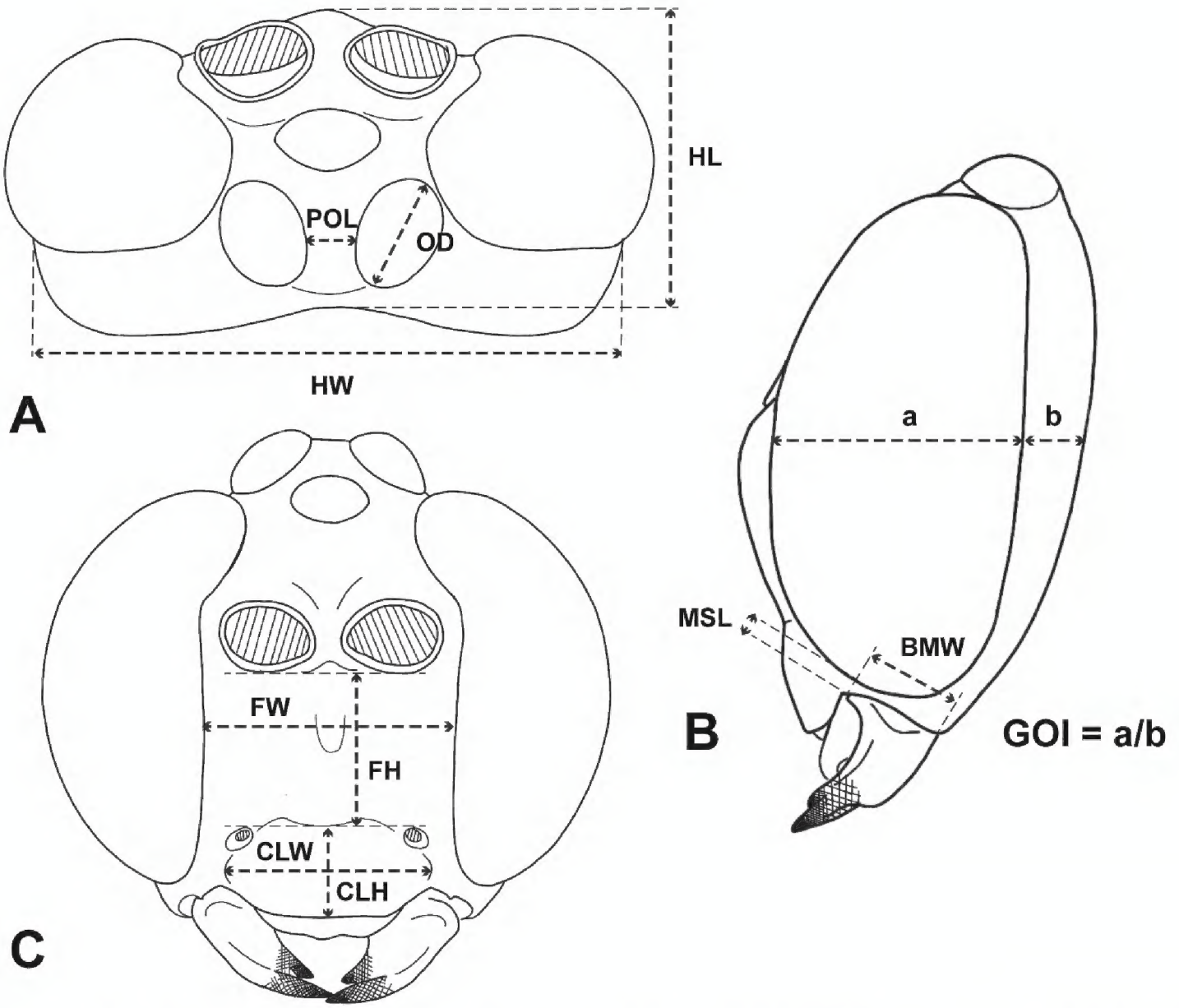

Figure 1. Schematic illustration of head measurements in the genus *Netelia* **A** head in dorsal view **B** head in anterior view **C** head in lateral view. Abbreviations: OD, lateral ocellus diameter; POL, postero-ocellar line; HL, length of head in dorsal view; HW, width of head in dorsal view; BMW, basal mandibular width in lateral view; MSL, length of malar space; GOI, geno-orbital index; FH, height of face; FW, width of face; CLH, height of clypeus; CLW, width of clypeus in anterior view.

Head in anterior view (Fig. 1C):

FH: height of face, the distance between lines of lower margins of antennal sockets and upper margin of tentorial pits; **FW:** width of face, minimum distance between each eye; **CLH:** height of clypeus, the distance between the upper groove and the ventral margin; **CLW:** width of clypeus.

Mesosoma and metasoma (Fig. 2A, B):

MSSL: length of mesoscutum in lateral profile; **MSSW:** width of mesoscutum in dorsal view; **SCL:** length of scutellum in lateral profile; **SCW:** anterior width of scutellum in dorsal view; **T:** metasomal tergite (length of metasomal tergite was measured in lateral profile, and the width was measured by maximum posterior width in dorsal view).

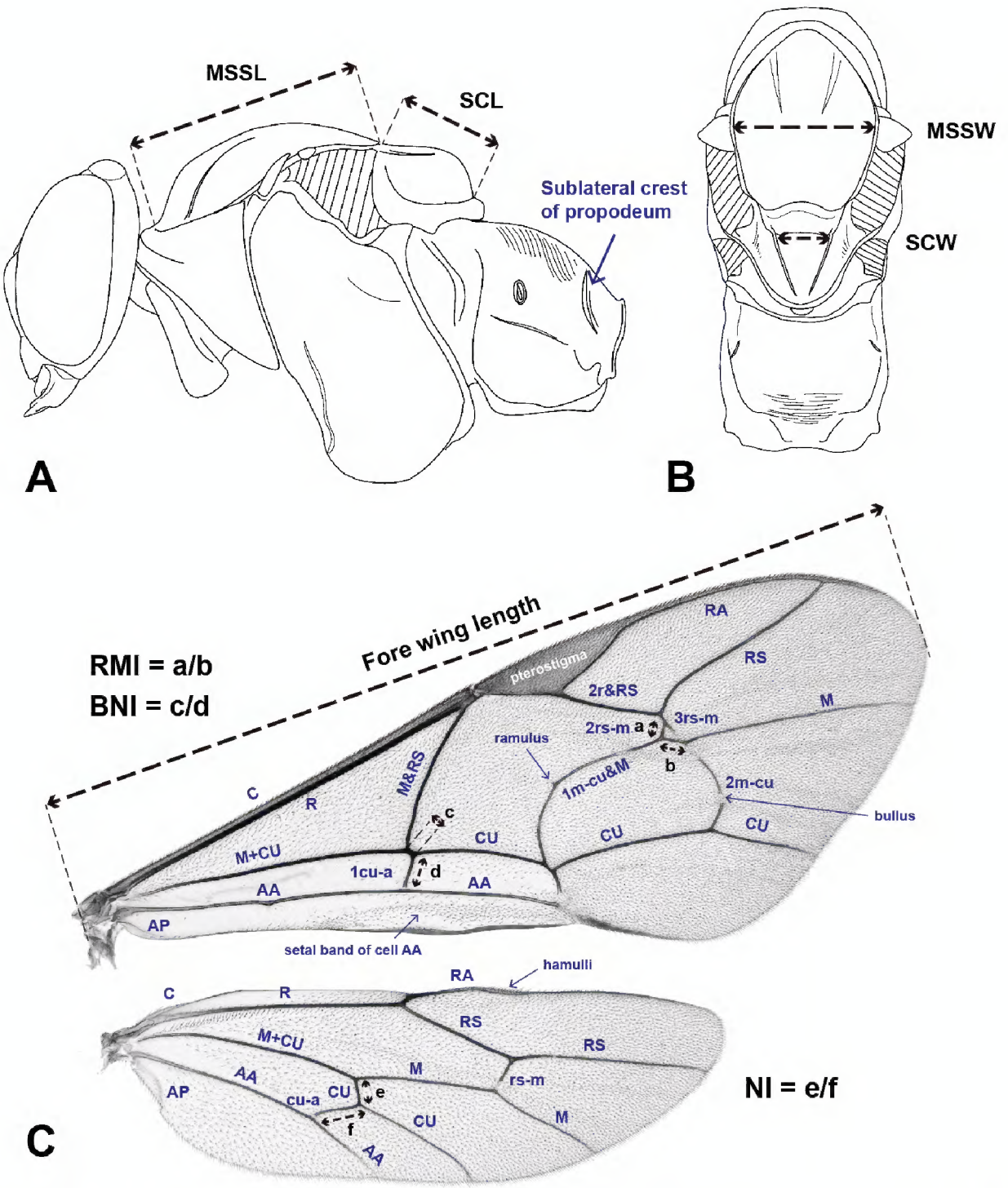

Figure 2. Schematic illustration of mesosoma and wing terminologies and measurements in the genus *Netelia* **A** mesosoma in lateral view **B** mesosoma in dorsal view **C** wings. Abbreviations: MSSL, length of mesoscutum in lateral profile; MSSW, width of mesoscutum in dorsal view; SCL, length of scutellum in lateral profile; SCW, anterior width of scutellum in dorsal view; RMI, radius-median index; BNI: basal-nervulus index; NI, nervellar index.

Wings (Fig. 2C):

RMI: radius-median index, $\frac{\text{length of fore wing 2rs-m}}{\text{length of fore wing M between 2rs-m and 2m-cu}}$;

BNI: basal-nervulus index, $\frac{\text{distance between fore wing M\&RS and 1cu-a}}{\text{length of fore wing 1cu-a}}$;

NI: nervellar index, $\frac{\text{length of hind wing CU between M and cu-a}}{\text{length of hind wing cu-a}}$

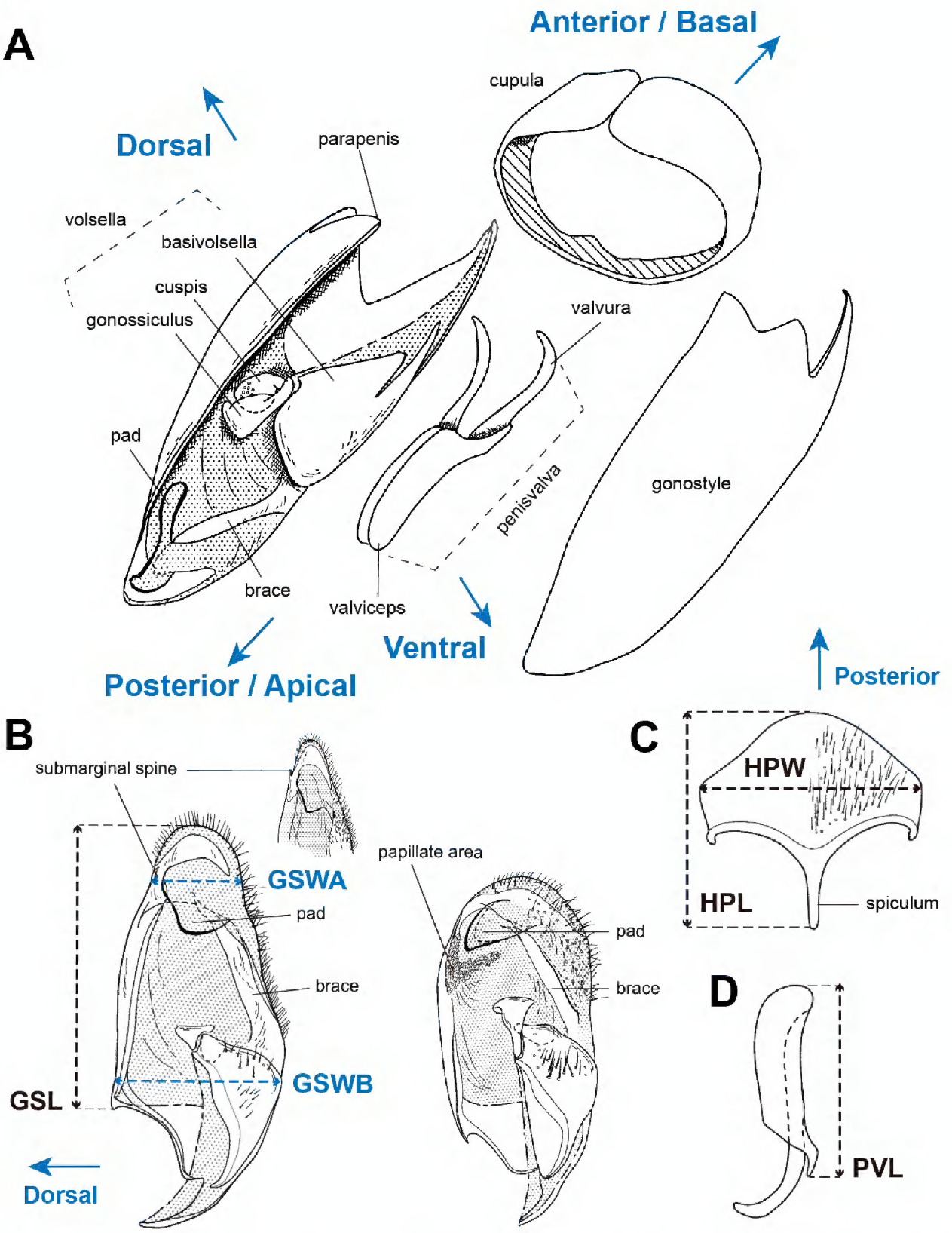

Figure 3. Schematic illustration of male genitalia terminologies and measurements in the genus *Netelia* **A** schematic drawing for general male genitalia of genus *Netelia* redrawn from Konishi (2005) **B** terminologies and measurements of gonostyle **C** measurements of abdominal sternum IX **D** measurements of penisvalva. Abbreviations: GSL, length of gonostyle; GSWA, apical width of gonostyle; GSWB, basal width of gonostyle; PVL, length of penisvalva; HPL, length of abdominal sternum IX (hypopygium); HPW, maximum width of abdominal sternum IX (hypopygium).

Male genitalia (Fig. 3):

GSL: length of gonostyle, measured by the distance between the parapenis and the apical point of the gonostyle; **GSWA:** apical width of gonostyle, measured at the base of the submarginal spine (if present); **GSWB:** basal width of gonostyle, measured at the ventral apex

of basivolsella; **PVL:** length of penisvalva, measured by the length of volviceps; **HPL:** length of abdominal sternum IX (hypopygium), measured from the apex of spiculum to the apex of posterior margin; **HPW:** maximum width of abdominal sternum IX (hypopygium).

The Latin term *ibidem*, meaning "same as previous except as follows" and abbreviated as 'ibid' was used to compress the locality information of materials examined. In the descriptions, the minimum and maximum values of measurements or ratios are connected by an en dash, followed by the mean plus-minus standard deviation in parentheses; when available, the value for the holotype is given in brackets. Measurements in the main text are rounded to one decimal place, whereas their means and standard deviations are calculated and rounded to two decimal places.

Morphological observations

Specimens were examined and measured by using a microscope LEICA S8APO (Leica Microsystems, Wetzlar, Germany) with a XFCAM autofocus CCD (Jet measurements, Taipei, Taiwan). Photographs were taken by a LEICA DMC5400 camera equipped with LEICA Z16 APO lens and LAS V4.13 auto-stacking system (Leica Microsystems, Wetzlar, Germany). In this study, all line drawings were created using Procreate (Savage Interactive, Australia) via iPad Air 4 (Apple Inc., USA). All figures were edited and arranged into figure plates using Adobe Illustrator CC and Photoshop CC (Adobe Systems Inc., San Jose, CA, USA).

Townes (1939) first utilized a method for dissecting and preserving male genitalia of *Netelia*, involving maceration in 10% sodium or potassium hydroxide, dissection in water, fixation and dehydration in 95% alcohol, and final mounting on a slide with Euparal. Townes' approach has been widely adopted by subsequent researchers (e.g., Delrio 1975; Kaur and Jonathan 1979; Tolkanitz 1981a; Konishi 1985, 2005), each implementing their own modifications. While Delrio and Kaur and Jonathan mounted the genitalia on slides in mounting media, Tolkanitz affixed them to a paper card by gel, and Konishi preserved them in a microvial with glycerol (as per Andersson (1972)). Considering the need to observe the gonostyles from multiple angles, especially in species with a submarginal spine on the gonostyle, we applied Konishi's method.

In this study, the male genitalia were dissected and macerated in 20% KOH solution for 1.5 hours at 65 °C, or in the buffer ATL with proteinase K (DNeasy Blood and Tissue Kit (QIAGEN, Hilden, Germany)) that can extract their DNA simultaneously. The dissected genitalia were preserved in a microvial with glycerol.

Improving male genitalia observation

Maceration can sometimes make the pad become translucent and difficult to interpret its shape (Fig. 4A). To improve the observation of membranous structures, this study developed two methods: (1) placing black paper or flannel as a background or adjusting the transmitted light source to enhance pad visibility (Fig. 4B), and (2) staining one side of the gonostyles using ink from a black rollerball pen by immersing it in a droplet of undiluted ink (or other dye such as chlorazol black E) for a few seconds,

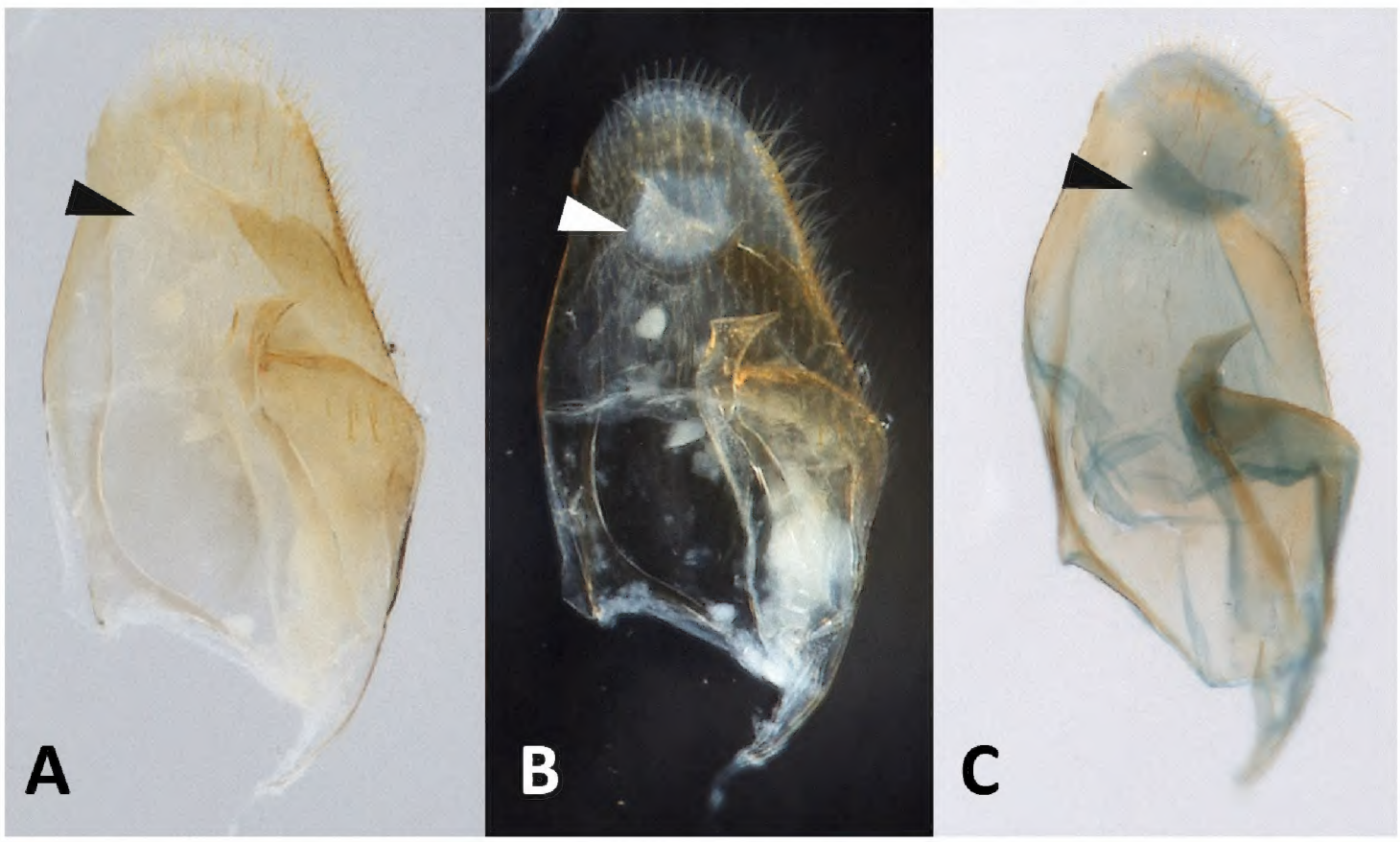

Figure 4. Gonostyles of male genitalia in *Netelia* observed using different methods. Triangles indicate the pad (*Netelia* (*Paropheltes*) *dalupalringi* sp. nov.) **A** unstained under light background **B** unstained under dark background **C** stained by ink of roller ball pen. Specimen: **A–B** CHP01409, holotype; **C** NMNS ENT 7470-233, paratype.

then washing it in water (Fig. 4C). If the genitalia are over-macerated in KOH, the use of a dark background becomes less effective, making staining a more suitable option.

The use of different observation methods enhances the visibility of various genital structures. For example, a transmitted light source improves the visibility of setae and sclerite shapes, while a dark background highlights membranous structures, such as the pad. To provide a comprehensive representation of genital morphology in *Netelia*, line drawings are recommended. In male genitalia illustrations here, stippling indicates membranous structures, short dashed lines denote structures covered by the membrane or cuticles, long-short dashed lines outline membranous structures (excluding the pad), and bold lines highlight the pad's outline.

Taxon sampling for molecular analysis

To expand taxon sampling for phylogenetic reconstruction and enhance species delimitation results, *COI* sequences of *Netelia* from worldwide records were retrieved from the BOLD systems. Sequences were selected from Barcode Index Number (BIN) clusters, with up to five sequences per cluster, each from a different locality. A total of 428 *COI* sequences from 190 BIN clusters were obtained from BOLD, forming the "BOLD dataset."

For phylogenetic reconstruction, the outgroups included the sister genus of *Netelia*, *Phytodietus* Gravenhorst, 1829, represented by three operational taxonomic units

(OTUs): *Phy. lindus* Gauld, 1997 [ACGBA3472-13], *Phy. obscurus* (Ratzeburg, 1852) [AGAKS1338-17], and *Phy. vulgaris* Cresson, 1870 [HQ107713]. *Neorhacodes* Hedicke, 1922 (*Neorhacodes enslini* (Ruschka, 1922) [MK959446]), the sister genus of Phytodietini (*Netelia* plus *Phytodietus*) or Phytodietini plus remaining ichneumonids (Bennett et al. 2019), was also included in the outgroups as the root of the tree. The "ALL (all-included) dataset," comprising the sequences of Taiwanese *Paropheltes*, the BOLD dataset, and outgroup OTUs, was constructed to test the monophyly of the subgenus *Paropheltes* and to perform species delimitation. Additionally, the "PARO (*Paropheltes*) dataset," consisting solely of species within the subgenus *Paropheltes*, including Taiwanese *Paropheltes* and sequences retrieved from the BOLD dataset (identified based on attached habitus photographs) and the outgroups, was also constructed for species delimitation analysis. The detailed sample information is provided in Suppl. material 1.

Laboratory procedure and quality control

Total genomic DNA was extracted using the DNeasy Blood and Tissue Kit (QIAGEN, Hilden, Germany), following the manufacturer's protocol or the non-destructive protocol proposed by Cruaud et al. (2019). Especially, the right mid leg or the male genitalia was removed from the specimen and preserved in 95% EtOH. The leg was cut into small pieces using sterile dissecting scissors before DNA extraction, while the male genitalia were soaked in buffer solution (180 µL of buffer ATL + 20 µL of proteinase K of DNeasy Blood and Tissue Kit) for at least 3 hours at 55 °C to preserved them through a non-destructive protocol. The volume of extracted DNA ranged from 25 to 100 µL, depending on the sample size.

In this study, the mitochondrial cytochrome c oxidase I (*COI*) gene, a widely used DNA marker for molecular identification and species delimitation in animals (Hebert et al. 2003a, 2003b, 2004; Hajibabaei et al. 2007), was employed for species delimitation. The primers pairs LCO1490 and HCO2198 (Folmer et al. 1994), and Ich_COI_F and Ich_COI_R (Chen et al. 2023), or their 1:1 cocktail were used for PCR amplification. PCR conditions were 4 min at 95 °C as an initial denaturation step, 35 cycles of 30 s at 95 °C for denaturation step, 1 min at 46 °C (or 45 °C) for annealing step, and 45 s at 72 °C for extension step, follow by a final extension step at 72 °C for 10 min. Each PCR was carried out in a 15 µL volume containing 4.3 µL sterile distilled water, 0.6 µL of each primer (10 µM), 7.5 µL of GoTaq® Green Master Mix (Promega, Madison, WI, USA) and 2.0 µL of DNA template. All the PCR products were purified and sequenced at Tri-I Biotech Inc. (Taipei, Taiwan).

For the quality control of sequences, chromatograms of each sequence were carefully examined using Codoncode Aligner ver. 10.0.2 (CodonCode Corporation, Dedham, MA, USA), and sequences displaying chaotic chromatograms or double peaks were excluded from the following analyses. Subsequently, the sequences were checked using BLAST (Altschul et al. 1990) to identify potential contamination from endosymbiont bacteria or other sources. Automatic multiple sequence alignments were then conducted in MAFFT ver. 7 on the website https://mafft.cbrc.jp/alignment/server/ (Katoh et al. 2019), where the default setting with 'Adjust direction according to the

first sequence' was applied to the datasets. The aligned *COI* dataset was finally translated into an amino acids' alignment using MEGA11 (Tamura et al. 2021) to detect pseudogenes based on stop codons or abnormal amino acid sequences.

Phylogenetic reconstruction and species delimitation

The datasets were initially partitioned by codon positions, and ModelFinder (Kalyaanamoorthy et al. 2017) implemented in the IQ-TREE program was then employed with the "partition merging" setting to search for the most suitable substitution model and partitioning scheme under both corrected Akaike information criterion (AICc) and the default setting Bayesian information criterion (BIC). The results of both methods were compared and choose the appropriate result for subsequent analyses. The maximum likelihood (ML) phylogenetic trees were reconstructed using the program IQ-TREE ver. 2.4.0 (Minh et al. 2020). Nodal supports were assessed with ultrafast bootstrap approximation (UFBoot2) (Hoang et al. 2017) and SH-like approximate likelihood ratio test (SH-aLRT) (Guindon et al. 2010) based on default parameter setting in the IQ-TREE program. The nodes with SH-aLRT ≥ 80% and UFBoot ≥ 95% for ML trees were considered strongly supported.

Two molecular species delimitation methods, Assemble Species by Automatic Partitioning (ASAP) (Puillandre et al. 2021) and Bayesian-based Poisson Tree Processes (bPTP) (Zhang et al. 2013), were applied for the ALL and PARO datasets in this study. Both datasets and their ML phylogenetic trees were employed for ASAP and bPTP analyses, respectively. These analyses were performed using online interfaces (ASAP: https://bioinfo.mnhn.fr/abi/public/asap/ and bPTP: https://species.h-its.org/), with ASAP relying on pairwise K2P genetic distances and bPTP based on unrooted trees. The results of molecular species delimitation were used to test the species hypothesis reconstructed by morphological evidence.

Results

Molecular data

For Taiwanese *Paropheltes* species, *COI* sequences of ten specimens belonging to three species were successfully amplified by PCR (see first ten rows in the file Suppl. material 1). The summary of both ALL and PARO datasets, including the information on the average length of unaligned sequences, length of aligned sequences, number of variable and parsimony-informative sites, and percentage of GC content, is provided in Table 1. For the substitution model selection in the following analyses, we adopted the BIC-based results for both the PARO and ALL datasets, as both criteria showed similar results for the smaller PARO dataset, whereas the model selected for the larger ALL dataset better explains the sequence variation within that dataset. The original alignment files and results are provided in Suppl. material 2 (the files named "Aln_[name of dataset].fas" contain the alignments for

Table 1. Summary of each aligned and trimmed molecular dataset including the information on the aligned length of sequences, average length of aligned sequences, number of variable and parsimony-informative (Pars-Inf) sites, and percentage of GC content.

	Number of sequences	Aligned length	Average length	Variable sites	Pars-Inf sites	GC (%)
ALL	442	624	610.9	384	361	29.5
PARO	37	624	611.2	286	253	28.2

each dataset, while the files named "Par_[name of dataset]_best_scheme ([model selection criterion]).nex" contain the best partitioning schemes and substitution models for the respective datasets).

Species delimitation

Fig. 5A presents the species delimitation results mapped onto the ML phylogenetic tree of PARO dataset, reconstructed using the TN+F+G4 substitution model partitioned by codon position (first plus second versus third). In the *COI* tree of the PARO dataset, each *Paropheltes* OTU forms a distinct lineage with strong nodal supports (Fig. 5A). The optimal partition in the ASAP analysis using the ALL dataset yielded a threshold K2P distance of 0.13731, while the optimal ASAP result of the PARO dataset delimited a higher threshold distance of 0.26493. All mean K2P pairwise distances between the *Paropheltes* OTUs in the PARO dataset exceed 0.05, with most values exceed 0.15, supporting their delimitation as separate species (Table 2). The bPTP analysis results are consistent with those of ASAP and the morphology. Based on morphological comparisons with type specimens, original and subsequent descriptions, and illustrations of the subgenus *Paropheltes* from worldwide localities, five species are recorded from Taiwan.

COI-based phylogeny

Fig. 5B presents the ML phylogenetic tree of the ALL dataset, reconstructed using the GTR+F+I+G4 substitution model without partitioning. Lineages labeled red represent OTUs belonging to the subgenus *Paropheltes*, identified either by examining directly the specimens, based on the habitus photos retrieved from the BOLD system (based on the distinct yellowish-white marking on the mesopleuron and the shape of the gonostyles), or based on the identification of sequences whose considered reliable. The genus *Netelia* forms a strongly supported clade (SH-aLRT/UFBoot = 96.4/100; Fig. 5B). However, the subgenus *Paropheltes* is recovered as polyphyletic, with *N. guptai* Kaur & Jonathan, 1979, *N. millieratae* (Kriechbaumer, 1897), *N. inedita* (Kokujev, 1899) (=*N. thomsoni* (Brauns, 1889)), *N. caucasica* (Kokujev, 1899), and BOLD:ACM9187 each forming a strongly supported independent lineage; *N. fulginosa*, *N. savchenkoi*, and *N. dalupalringi* sp. nov. are clustering together, but the clade is not strongly supported, while a clade of three OTUs (*N. tarsata*, BOLD: AAH2123, and BOLD: ACF7679) is strongly supported (SH-aLRT/UFBoot = 99.3/100) (Fig. 5B; Suppl. material 2).

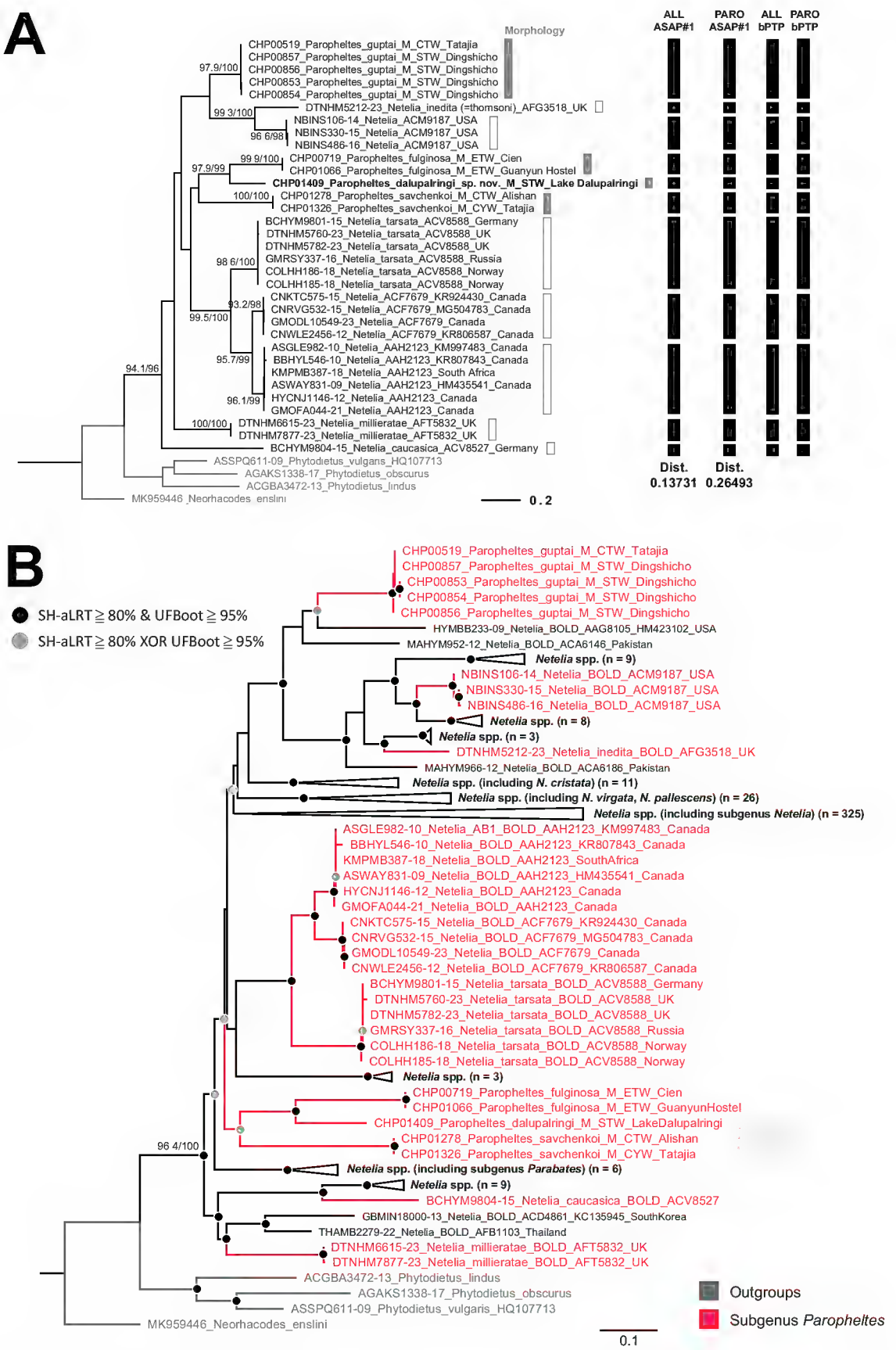

Figure 5. *COI*-based species delimitation and phylogeny of the genus *Netelia*, subgenus *Parapheltes* **A** maximum Likelihood (ML) phylogenetic tree of PARO dataset, mapped with species delimitation results using ALL and PARO datasets as black bars, as well as the threshold K2P distance for the ASAP results. Nodal support values are expressed as SH-aLRT/UFBoot percentages (%). Support values with SH-aLRT/UFBoot both < 80/95 are not shown. Gray bars mapped on each clade indicate morphospecies, while blank bars represent cases where detailed morphological data are unavailable **B** *COI*-based ML tree of world *Netelia* reconstructed using ALL dataset with most non-*Parapheltes* clades collapsed. Circles on the nodes represent different degrees of 'SH-aLRT/UFBoot percentages (%), and clades with both support values < 80/95 are not shown. Outgroups are labeled gray, while the operative taxonomic units of subgenus *Parapheltes* are highlighted in red. Branch lengths of both phylogenetic trees are proportional to the infer number of nucleotide substitutions per site. The complete trees are provided in Suppl. material 3 (the .treefile and .pdf files) Abbreviations: M: male; CTW: central Taiwan; STW: southern Taiwan; ETW: eastern Taiwan.

Table 2. Mean Pairwise K2P distance (lower-left) and standard deviations estimated by 100 replications of Bootstrap (upper-right) of *COI* sequences of the operative taxonomic units (OTU) of subgenus *Paropheltes* included in this study.

	N. caucasica	***N. fulginosa***	***N. guptai***	***N. inedita* (= *thomsoni*)**	***N. millieratae***	***N. savchenkoi***	***N. tarsata***	***N. dalupalringi* sp. nov.**	**BOLD: ACM9187**	**BOLD: ACF7679**	**BOLD: AAH2123**
N. caucasica		0.0251	0.0216	0.0258	0.0216	0.0259	0.0218	0.0214	0.0226	0.0201	0.0209
N. fulginosa	0.2520		0.0201	0.0198	0.0200	0.0207	0.0193	0.0174	0.0204	0.0178	0.0185
N. guptai	0.2129	0.2124		0.0174	0.0165	0.0205	0.0183	0.0180	0.0177	0.0199	0.0199
N. inedita (= *thomsoni*)	0.2423	0.2124	0.1959		0.0202	0.0230	0.0219	0.0184	0.0168	0.0230	0.0210
N. millieratae	0.1836	0.1946	0.1594	0.2122		0.0191	0.0179	0.0178	0.0204	0.0194	0.0194
N. savchenkoi	0.2410	0.2012	0.1860	0.2335	0.1877		0.0201	0.0213	0.0219	0.0209	0.0206
N. tarsata	0.2203	0.2156	0.1686	0.2481	0.1638	0.1913		0.0175	0.0206	0.0124	0.0142
N. dalupalringi sp. nov.	0.1964	0.1518	0.1734	0.1820	0.1695	0.2009	0.1669		0.0192	0.0180	0.0184
BOLD:ACM9187	0.2263	0.2173	0.1457	0.1475	0.1893	0.2170	0.2083	0.1873		0.0213	0.0216
BOLD:ACF7679	0.1840	0.1841	0.1834	0.2174	0.1530	0.1942	0.1040	0.1719	0.1969		0.0093
BOLD:AAH2123	0.1953	0.2038	0.1817	0.2317	0.1669	0.1821	0.1072	0.1816	0.2051	0.0506	

The complete phylogenetic trees are provided in Suppl. material 2 (the files named "[name of dataset].treefile" and "[name of dataset].pdf" contain the complete phylogenetic trees; and "[name of dataset].log" is the log file for the phylogenetic reconstruction).

Taxonomy

The five Taiwanese species include four previously described species—*Netelia* (*Paropheltes*) *fulginosa* Konishi, 1996, *N.* (*Paro.*) *guptai* Kaur & Jonathan, 1979, *N.* (*Paro.*) *savchenkoi* Tolkanitz, 1981, and *N.* (*Paro.*) *yui* Konishi, 2000—as well as a new species *N.* (*Paro.*) *dalupalringi* Chen, Konishi & Shiao, sp. nov.

Among them, the independent species status of *N.* (*Paro.*) *fulginosa*, *N.* (*Paro.*) *guptai*, *N.* (*Paro.*) *savchenkoi*, and *N.* (*Paro.*) *dalupalringi* sp. nov. is further supported by present *COI*-based species delimitation (Fig. 5A). Although molecular data were unavailable for *N.* (*Paro.*) *yui* herein, its distinct morphological characteristics support its recognition as independent species. Figs 6–17 illustrate the morphology of Taiwanese *Paropheltes*, with Suppl. material 3 summarizing their measurements. The original photographs of the male genitalia of Taiwanese *Paropheltes* are available in Suppl. material 4.

Family Ichneumonidae Latreille, 1802
Subfamily Tryphoninae Shuckard, 1840
Tribe Phytodietini Hellén, 1915
Genus *Netelia* Gray, 1860

Subgenus *Paropheltes* Cameron, 1907

Paropheltes Cameron, 1907: 1011. Type species: *Paropheltes flavolineatus* Cameron, 1907. By monotypy.

Diagnosis. Most species of this subgenus can be distinguished from other subgenera in having the combination of the following characters: occipital carina weak, present at least laterally; mesopleuron polished, minutely punctate; hind tarsal claw with pectens not extending beyond its apex; fore wing 1cu-a slightly basad, opposite, or slightly or far distad to M&RS; scutellum with lateral carina variable, from absent to extend to the apex. Konishi (1996a) stated that the heterogeneous male genitalia structures of this subgenus cannot be use as diagnostic characters of this subgenus.

However, several species been classified within *Paropheltes* or other subgenera make the subgeneric boundary ambiguous: some specimens of *N.* (*Paro.*) *fulginosa* Konishi, 1996 has its occipital carina completely absent, which makes these specimens difficult to distinguish from species of subgenus *Longiterebates*; *N.* (*N.*) *fulvator* Delrio, 1971 has its scutellum with lateral carina only extending to 0.3 of its length and therefore could be confused with *Paropheltes* (as other members of subgenus *Netelia* have lateral

carina of scutellum extending to the apex); some species have fore wing 1cu-a opposite to M&RS which can be confused with species of the subgenus *Prosthodocis*.

Species included. This subgenus comprises 46 valid species (Bennett 2015). This study first reports this subgenus from Taiwan, comprising five species. Among them, there are four described species and one new species.

Distribution. Worldwide, the genus comprises 11 species in the Nearctic, 26 in the Palearctic, six in the Oriental, five in the Afrotropical, and one in the Australasia regions (Bennett 2015; Yu et al. 2016). No species have been described from the Neotropical region (Bennett 2015).

Bionomics. The species of this subgenus mainly use Geometridae, especially *Eupithecia* species, as host (Brischke 1880; Morley 1915). Host records from Drepanidae (Brischke 1880) and Gelechiidae (Aubert et al. 1984) were considered unreliable (Bennett 2015).

Remarks. Townes (1939) subdivided this subgenus into five species groups: *N.* (*Paro.*) *flavolineata*, *N.* (*Paro.*) *barberi*, *N.* (*Paro.*) *tarsata*, *N.* (*Paro.*) *radiata*, and *N.* (*Paro.*) *ciliata* species groups. The classification was based on various morphological characters including the length of the lateral carina of the scutellum, the presence of the propodeal sublateral crest, the position of 1cu-a and M&RS, the margin of the pad, the length of the ovipositor, and the color pattern of the mesosoma. Subsequently, Kaur and Jonathan (1979) established two additional species groups, *N.* (*Paro.*) *thomsoni* and *N.* (*Paro.*) *guptai* species groups, based on the presence of a submarginal spine on the gonostyle, as well as the shape of the gonostyle and the characters of the pad and brace. Previous morphology-based phylogenetic studies (Coronado-Rivera 2009) have shown this subgenus to be polyphyletic, likely due to the highly heterogeneous morphology of the gonostyle. The *COI* phylogeny in this study (Fig. 5B) also supports the polyphyly of this subgenus.

Key to males of Taiwanese species of the subgenus *Parophelte*s

1 Gonostyle relatively simple, with brace shorter than half of gonostyle length apical to ventral apex of basivolsella, pad vestigial and apically rounded, and submarginal spine absent (Fig. 17G); fore wing vein 1cu-a far distad to M&RS with BNI > 0.6 (0.7–1.0); propodeal striation and sublateral crest strong; fore wing cell AA with setal band broad and parallel-sided (Fig. 17G); ground body coloration orange (Figs 6B, 9); head, lateral margin and area between lateral and median lobes of mesoscutum, posterior 0.3 of scutellum, and dorso-anterior corner of mesopleuron yellowish white (Fig. 9A–E) ..... ***N.* (*Paro.*) *guptai* Kaur & Jonathan, 1979**

– Gonostyle not simple, with pad and brace well developed, submarginal spine present or absent; fore wing vein 1cu-a basad or distad to M&RS with BNI < 0.5 (0.1–0.4); propodeal striation and sublateral crest not strong, sublateral crest absent in some species; fore wing cell AA with setal band narrow medially; ground body coloration yellowish brown or brown, lacking distinct yellowish white marking; head completely yellowish brown or brown **2**

2 Gonostyle with papillate area (Fig. 17C, N, O); pad tapered and pointed dorso-basally (Fig. 17C, D, N, O); ground body coloration usually brown (Fig. 6A, D) **3**

– Gonostyle without papillate area; pad not as above; ground body coloration yellowish brown **4**

3 Larger species, fore wing length > 9.0 (10.0–11.1) mm; occipital carina absent or with vestige dorsally; lateral ocelli almost touching eyes (Fig. 7B); propodeal sublateral crest strong (Figs 7D, 8G); gonostyle with papillate area weak, pad narrow (Fig. 17C); ocellar area, mesoscutum, and mesopleuron except speculum brown..... ***N.* (*Paro.*) *fulginosa* Konishi, 1996**

– Smaller species, fore wing length < 8.0 (6.2–7.2) mm; occipital carina present; lateral ocelli not touching eyes (Figs 12B, 13E); propodeal sublateral crest absent (Figs 12D, 13H); gonostyle with papillate area distinct, pad broader (Fig. 17N, O); ocellar area and mesoscutum black or blackish brown, mesopleuron yellowish brown to brown (Figs 6D, E, 12D, 13B) .... ***N.* (*Paro.*) *yui* Konishi, 2000**

4 Flagellum with 45–48 segments; occipital carina complete or absent dorsally; scutellum with lateral carina present on at least anterior 0.8; propodeal sublateral crests not connected dorsally (Fig. 10E); gonostyle slightly tapered apically, pad larger and rounded rectangular (Fig. 17J, K); submarginal spine of gonostyle short (Fig. 17K); penisvalva with valvura short and dorsally curved, not slender (Fig. 17I) ..... ***N.* (*Paro.*) *savchenkoi* Tolkanitz, 1981**

– Flagellum with 37–41 segments; occipital carina vestigial dorsally or completely absent; scutellum with lateral carina present on anterior 0.6; propodeal sublateral crests connected or almost connected dorsally (Fig. 15E); gonostyle blunt apically, pad smaller and semi-circular (Fig. 17R, S); submarginal spine of gonostyle long (Fig. 17S); penisvalva with valvura long and straight, slender (Fig. 17Q) .... ***N.* (*Paro.*) *dalupalringi* Chen, Konishi & Shiao, sp. nov.**

Key to females of Taiwanese species of the subgenus *Paropheltes*

(mostly based on the descriptions of Konishi (1996a) and Kaur and Jonathan (1979))

1 Fore wing vein 1cu-a far distad to M&RS; propodeal striation and sublateral crest strong; ground body coloration orange with distinct yellowish white markings on lateral margin and area between lateral and median lobes of mesoscutum, scutellum, and dorso-anterior corner of mesopleuron; head ground coloration yellowish white..... ***N.* (*Paro.*) *guptai* Kaur & Jonathan, 1979**

– Fore wing vein 1cu-a slightly basad or distad to M&RS; propodeal striation and sublateral crest not strong, sublateral crest absent in some species; ground body coloration yellowish brown or brown; head ground coloration yellowish brown or brown **2**

2 Mesoscutum completely blackish brown (in Taiwanese specimens); lateral ocelli not touching eyes; propodeal sublateral crest absent or weak..... ..... ***N.* (*Paro.*) *yui* Konishi, 2000**

– Mesoscutum yellowish brown to brown; lateral ocelli almost touching eyes (except some specimens of *N. dalupalringi* sp. nov.); propodeal sublateral crest present, usually strong.....**3**

3 Occipital carina complete or nearly complete but absent dorsally; lateral carina of scutellum present at least on anterior 0.8 .... ***N.* (*Paro.*) *savchenkoi* Tolkanitz, 1981**

– Occipital carina vestigial dorsally or completely absent; lateral carina of scutellum present at least on anterior 0.8 .....**4**

4 Ground color of temple, ocellar area, and mesopleuron brown; propodeal sublateral crest not extended and connected dorsally; fore and hind tarsal claws with 8–11 pectens (for Japanese specimens; Konishi 1996a) ....***N.* (*Paro.*) *fulginosa* Konishi, 1996**

– Ground color of temple, ocellar area, and mesopleuron (pale) yellowish brown (Fig. 16); propodeal sublateral crest extended and (almost) connected dorsally (Fig. 16E); fore and hind tarsal claws with 7–8 pectens..... .....***N.* (*Paro.*) *dalupalringi* Chen, Konishi & Shiao, sp. nov.**

***Netelia* (*Paropheltes*) *fulginosa* Konishi, 1996**
Figs 6A, 7, 8, 17A–D

Netelia (*Paropheltes*) *fulginosa* Konishi, 1996a: 173.

Diagnosis. This species can be distinguished from other species of subgenus *Paropheltes* in having the combination of the following characters: occipital carina completely absent in most specimens (Konishi 1996a), or with only a vestige dorsally in some specimens; propodeum with sublateral crest strong; gonostyle with submarginal spine dorso-apically; pad narrow and projected dorso-basally, with weak papillate area on apex of the pad; vertex, ocellar area, mesoscutum, scutellum, and dorsal surface of propodeum brown.

This species may be confused with species belonging to the subgenus *Longiterebates* due to the complete absence of the occipital carina in some specimens, as noted by Konishi (1996a). However, Konishi (1996a) restricted the true *Longiterebates* to India and described this species in subgenus *Paropheltes*. This species is most similar to *N.* (*Longiterebates*) *grandis* Kaur & Jonathan, 1979 in having strong propodeal sublateral crest, similar shape of gonostyle, and dorso-basally projected pad, but differs in *N.* (*Paro.*) *fulginosa* having weak papillate area on apex of the pad (lacking papillate area in *N.* (*Longiterebates*) *grandis*) (Konishi, 1996a).

Type material. ***Holotype.*** Japan • 1 ♂; Tokyo, Hinohara-mura, Yazawa; 14. VII. 1988; light trap ("at light"); H. Nagaoka leg.; Voucher: NARO (Fig. 8).

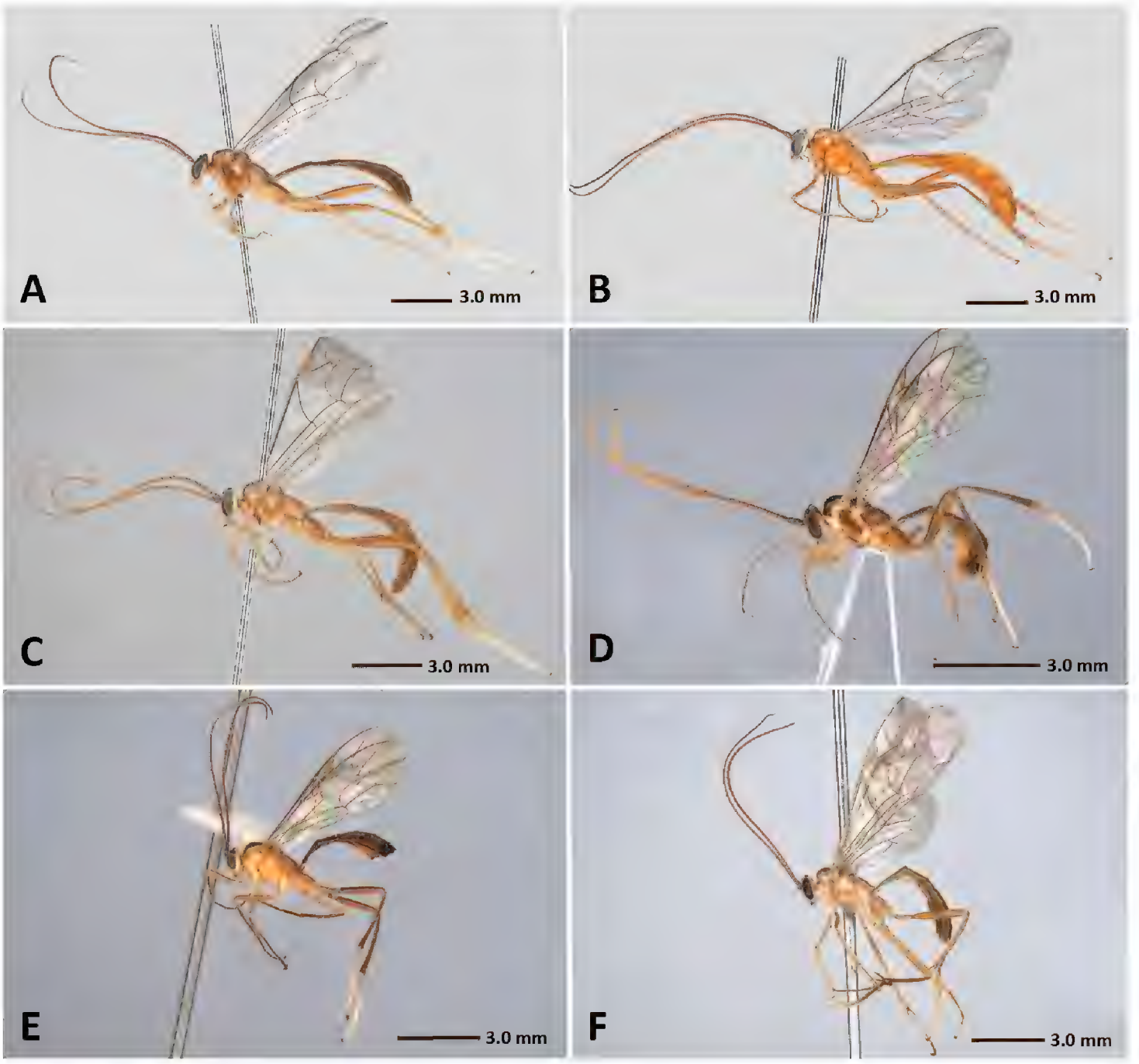

Figure 6. Habitus of males of Taiwanese species of subgenus *Paropheltes* **A** *Netelia* (*Propheltes*) *fulginosa* Konishi, 1996 (NMNS ENT 8951-10 (CHP00719)) **B** *N.* (*Paro.*) *guptai* Kaur & Jonathan, 1979 (NMNS ENT 8951-9 (CHP00519)) **C** *N.* (*Paro.*) *savchenkoi* Tolkanitz, 1981 (NMNS ENT 9068-2 (CHP01326)) **D** *N.* (*Paro.*) *yui* Konishi, 2000, Japanese specimen (KPMNH) **E** ditto, Taiwanese specimen (TARI Net12) **F** *N.* (*Paro.*) *dalupalringi* Chen, Konishi & Shiao, sp. nov. (NMNS ENT 9068-1 (CHP01409), holotype).

Non-type material. Taiwan – **Hualien County** • 1 ♂; Xiulin Township, Cien–Bilu giant tree; 27. V. 2020; light trap; C.-L. Huang, L.-H. Wang leg.; GenBank: PV910508 (*COI*); Sample ID: CHP00719; Voucher: NMNS ENT 8951-10. 1 ♂; Xiulin Township, Taroko National Park, Kuan-Yun Hostel; 30. V. 2020; light trap; K.-Y. Chen leg.; GenBank: PV910509 (*COI*); Sample ID: CHP01066; Voucher: NMNS ENT 8951-17. – **Nantou County** • 1 ♂; Ren'ai Township (Jenai), Nanshanchi; 17–19. V. 1999; UV light trap; W. T. Yang leg.; Voucher: NMNS ENT 3221-1153. 1 ♂; Ren'ai Township, Tayuling, 820 forest road ('820 Fogeste'); 2. IX. 2008; UV light trap; H. H. Lin leg.; Voucher: NMNS ENT 6070-581. 1 ♂; Ren'ai Township, Meifeng; 11. IX. 2002; Mercury light; C.S. Lin, W.T. Yang leg.; Voucher: NMNS ENT 3940-50.

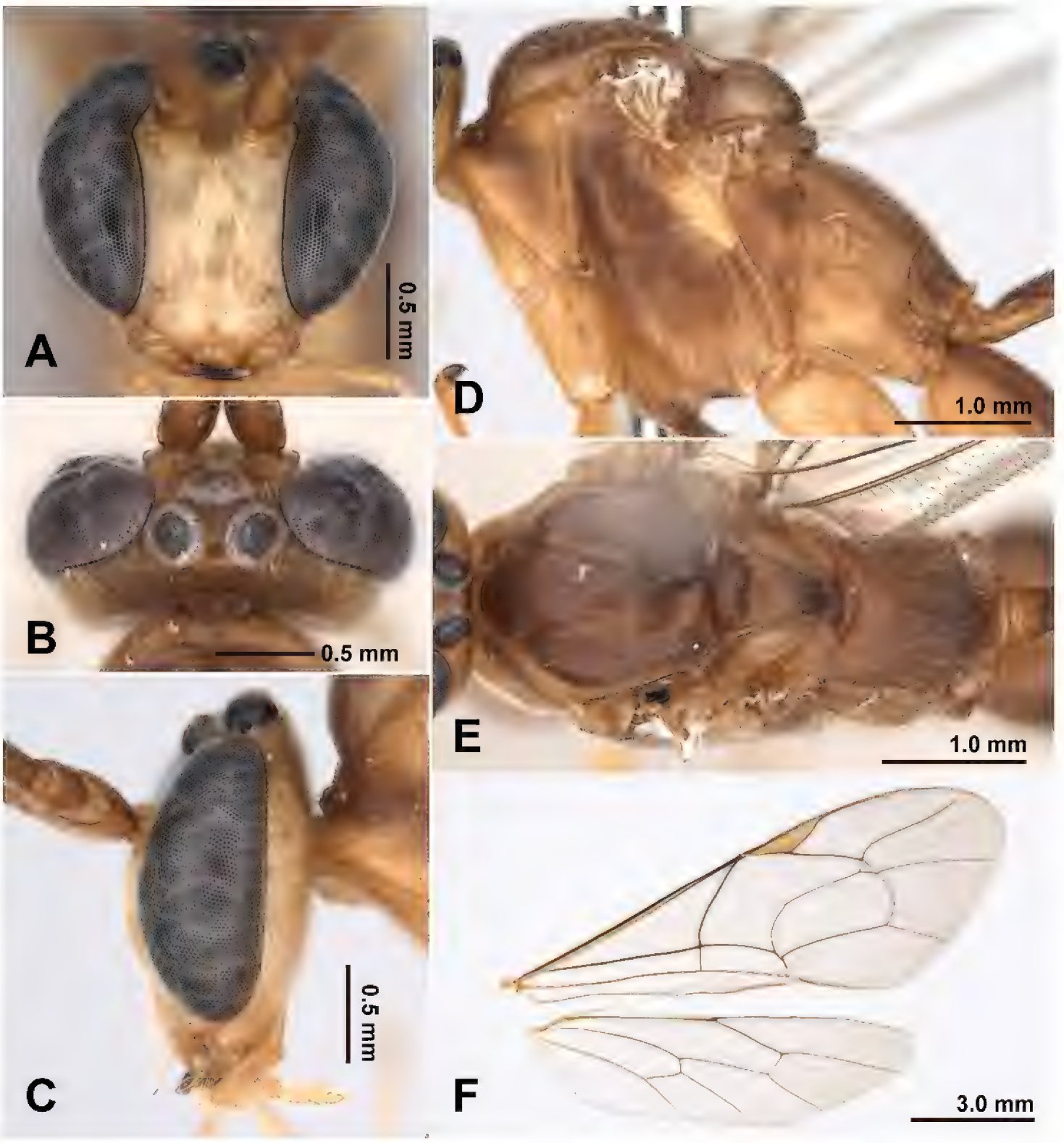

Figure 7. Taiwanese specimens of *Netelia* (*Paropheltes*) *fulginosa* Konishi, 1996 (male) **A** head in anterior view **B** head in dorsal view **C** head in lateral view **D** mesosoma in lateral view **E** mesosoma in dorsal view **F** wings. Specimen: **A, C–F** NMNS ENT 8951-10 (CHP00719); **B** NMNS ENT 8951-17 (CHP01066).

1 ♂; Ren'ai Township, Sungkang; alt. 2100 m; X. 1985; Malaise trap; K. S. Lin leg.; Voucher: TARI Net 59.

Redescription based on Taiwanese specimens. Measurements were based on 5 males. **Male.** ***Head*** (Figs 7A–C, 8C–E): vertex polished and smooth; frons, face, clypeus matt and finely coriaceous with setae; HW/HL = 1.6–2.1 (1.85 ± 0.21); lateral ocelli almost touching eyes, OD = 0.2–0.3 (0.25 ± 0.03) mm, POL/OD = 0.3–0.5 (0.42 ± 0.06); occipital carina vestigial dorsally; face with FW/FH = 1.1–1.3 (1.13 ± 0.08); clypeus CLW/CLH = 1.7–2.1 (1.88 ± 0.18), ventral margin truncated

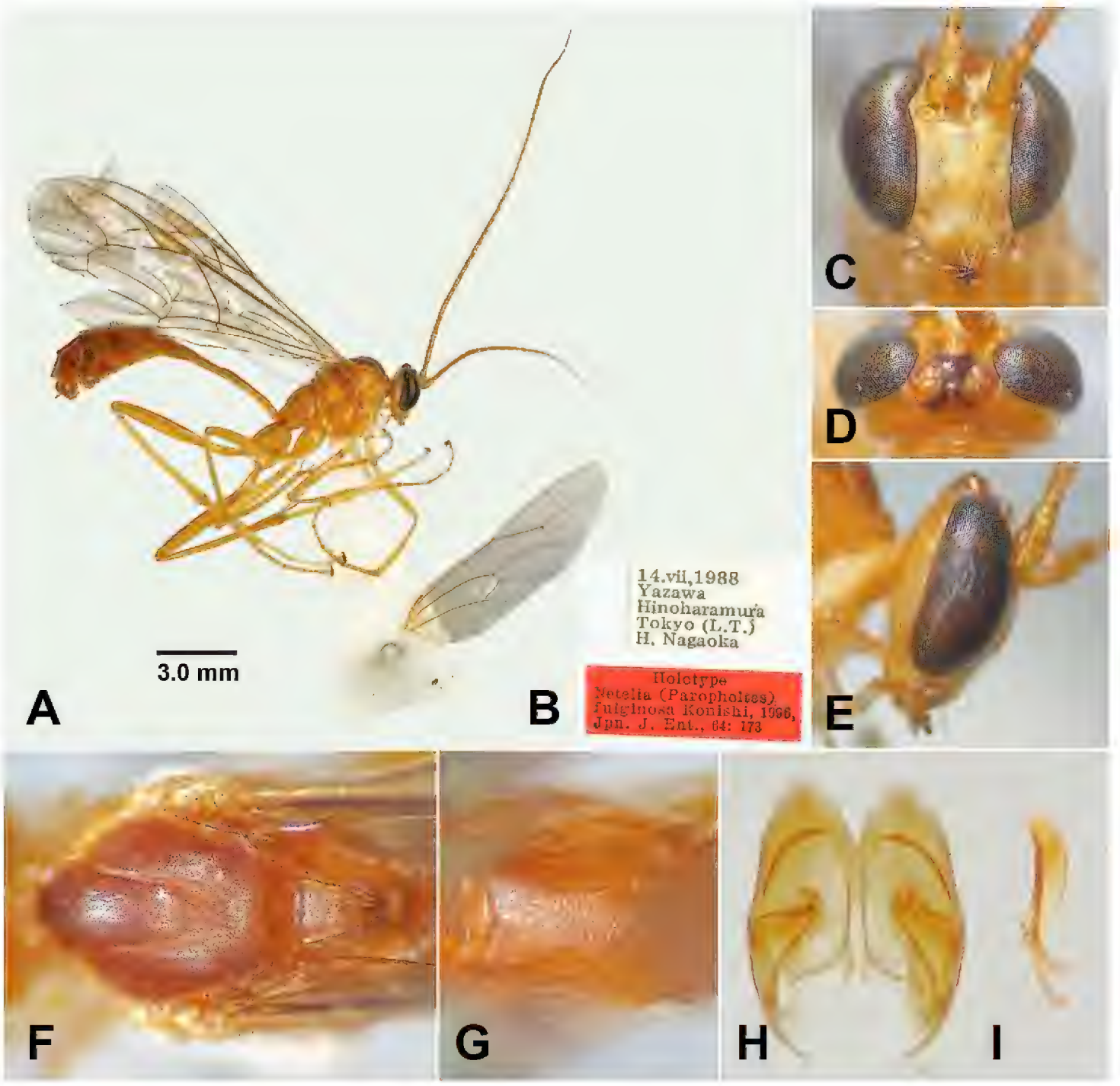

Figure 8. Holotype of *Netelia* (*Paropheltes*) *fulginosa* Konishi, 1996 (NARO, male) **A** lateral habitus **B** labels **C** head in anterior view **D** head in dorsal view **E** head in lateral view **F** mesosoma and scutellum in dorsal view **G** propodeum in dorsal view **H** gonostyles **I** penisvalva.

or slightly concave; malar space with MSL/BMW = 0.2–0.4 (0.32 ± 0.06); gena GOI = 3.0–4.0 (3.35 ± 0.42); flagellum with 40–44 segments, 1st flagellomere 1.1–1.5 (1.34 ± 0.15) × as long as 2nd flagellomere, 4.3–5.5 (4.74 ± 0.48) × as long as wide.

Mesosoma (Figs 7D, E, 8F, G): pronotum, mesoscutum, and scutellum matt, coriaceous or finely coriaceous; mesopleuron polished, coriaceous with even and minute punctures; pronotum with rugae on middle area, epomia absent; mesoscutum MSSL/MSSW = 1.1–1.3 (1.16 ± 0.08), with notaulus present on about anterior 0.6; scutellum SCL/SCW = 1.2–1.9 (1.55 ± 0.29), with lateral carina present on anterior 0.5; propodeum evenly and minutely punctate on anterior 0.3, with weak and transverse striae posteriorly, sublateral crest strong but not extended and connected dorsally.

Wings (Fig. 7F): fore wing length 9.8–11.1 (10.45 ± 0.57) mm; 3rs-m present, areolet large and anteriorly pointed; 2rs-m and abscissa between 2rs-m and 2m-cu in acute angle, RMI = 0.7–0.8 (0.73 ± 0.06); ramulus absent; 1cu-a straight or slightly curved posteriorly, vertical, almost opposite (slightly basad) to M&RS with BNI = 0.1–0.2 (0.11 ± 0.03); cell AA with setal band narrow on about proximal 0.3 and strongly broad distally; AA almost straight; hind wing with 5–6 distal hamuli; NI = 0.3–0.5 (0.38 ± 0.07).

***Legs*:** fore tibial spur 0.4 (0.37 ± 0.02) × as long as 1st tarsomere; fore 1st tarsomere 13.8–19.1 (16.20 ± 2.18) × as long as wide, 1.6–1.8 (1.76 ± 0.08) × as long as 2nd; fore tarsal claw with 20–22 pectens; hind 1st tarsomere 13.1–15.9 (14.58 ± 1.09) × as long as wide, 1.9–2.1 (1.95 ± 0.09)× as long as 2nd; hind tarsal claw normal, with 18–19 pectens.

Metasoma (Figs 8H, I, 17A–D): T1 slender, 4.2–5.2 (4.78 ± 0.37) × as long as posterior width, 1.5–1.6 (1.53 ± 0.06) × as long as T2; abdominal sternum IX HPW/HPL = 0.9–1.0 (0.99 ± 0.03), posteriorly convex; gonostyle rounded apically, with submarginal spine present on about dorso-apical 0.1, GSWA/GSL = 0.3 (0.30 ± 0.02), GSWB/GSL = 0.5–0.6 (0.56 ± 0.03), pad long and narrow, located dorso-apically and projected dorso-basally; brace parallel-sided; with weak papillate area on apex of pad; gonossiculus strongly broad apically and pointed ventrally; basivolsella with patch of dense, slender seta; penisvalva with PVL/GSL = 0.5–0.6 (0.54 ± 0.04), volviceps with dorsal margin about 0.8 length of ventral margin, valvura dorsally curved and slender.

Coloration (Figs 6A, 7, 8A): head brown, except face and clypeus yellowish white; mesosoma brown, except anterior and posterior corners of pronotum, lateral margin of mesoscutum, and speculum of mesopleuron yellow; wings hyaline, with wing vein blackish brown and pterostigma pale yellowish brown; legs brown, except hind tarsi yellowish white; metasoma brown.

Female. Taiwanese specimens not examined. Described in Konishi (1996a).

Distribution. Japan (Honshu [type locality], Shikoku, Kyushu (Konishi, 1996a)), Taiwan (new record: Hualien, Nantou).

Bionomics. Unknown.

Remarks. The occipital carina of the Taiwanese specimens is vestigial dorsally, differing from most type specimens of this species in which the occipital carina is absent, though this character state falls within the known variation range of the species (Konishi 1996a). This species cannot be assigned to any species group of this subgenus.

Netelia (*Paropheltes*) *guptai* Kaur & Jonathan, 1979

Figs 6B, 9, 17E–G

Netelia (*Paropheltes*) *guptai* Kaur & Jonathan, 1979: 201.

Diagnosis. This species can be distinguished from other species of subgenus *Paropheltes* in having the combination of the following characters: fore wing cell AA with setal band broad; propodeum with striation and sublateral crest strong; gonostyle with pad

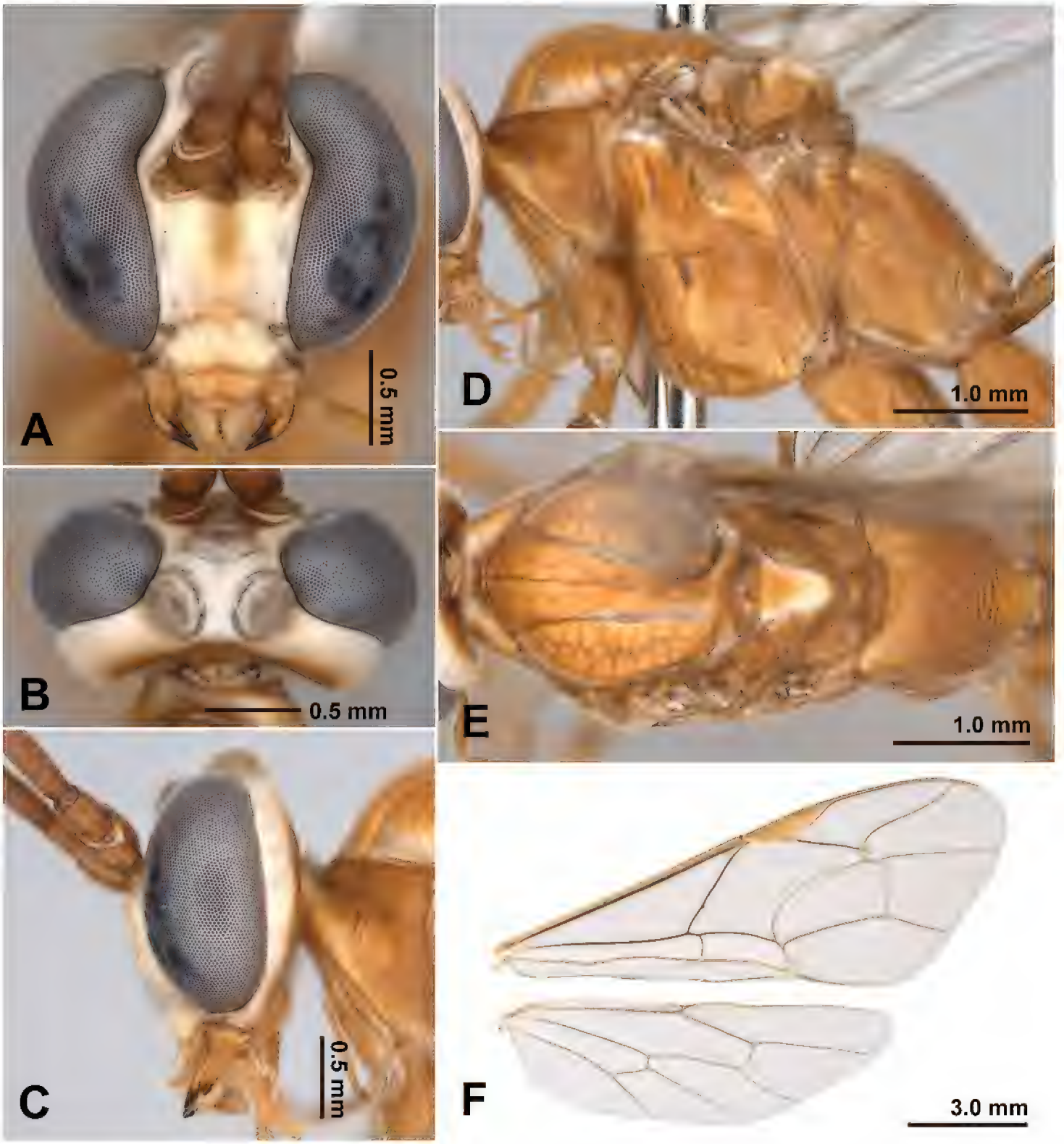

Figure 9. Taiwanese specimen of *Netelia* (*Paropheltes*) *guptai* Kaur & Jonathan, 1979 (male) **A** head in anterior view **B** head in dorsal view **C** head in lateral view **D** mesosoma in lateral view **E** mesosoma in dorsal view **F** wings. Specimen: **A–F** NMNS ENT 8951-16 (CHP00854).

vestigial, located medially and projected dorso-basally, forming weak membranous overhang; submarginal spine absent; brace shorter than half of gonostyle length apical to ventral apex of basivolsella; head ground coloration yellowish white, and mesosoma orange with yellowish white marking on mesoscutum (lateral margin and area between the lateral and median lobes) and scutellum (about posterior 0.3).

Non-type material. Taiwan – **Nantou County** • 1 ♂; Xingyi Township, Tatajia, Tai-18th highway 100.5 k, 23.480555°N, 120.852519°E; 16. VI. 2020; light trap; C.-L. Huang leg.; GenBank: PV910503 (*COI*); Sample ID: CHP00519; Voucher:

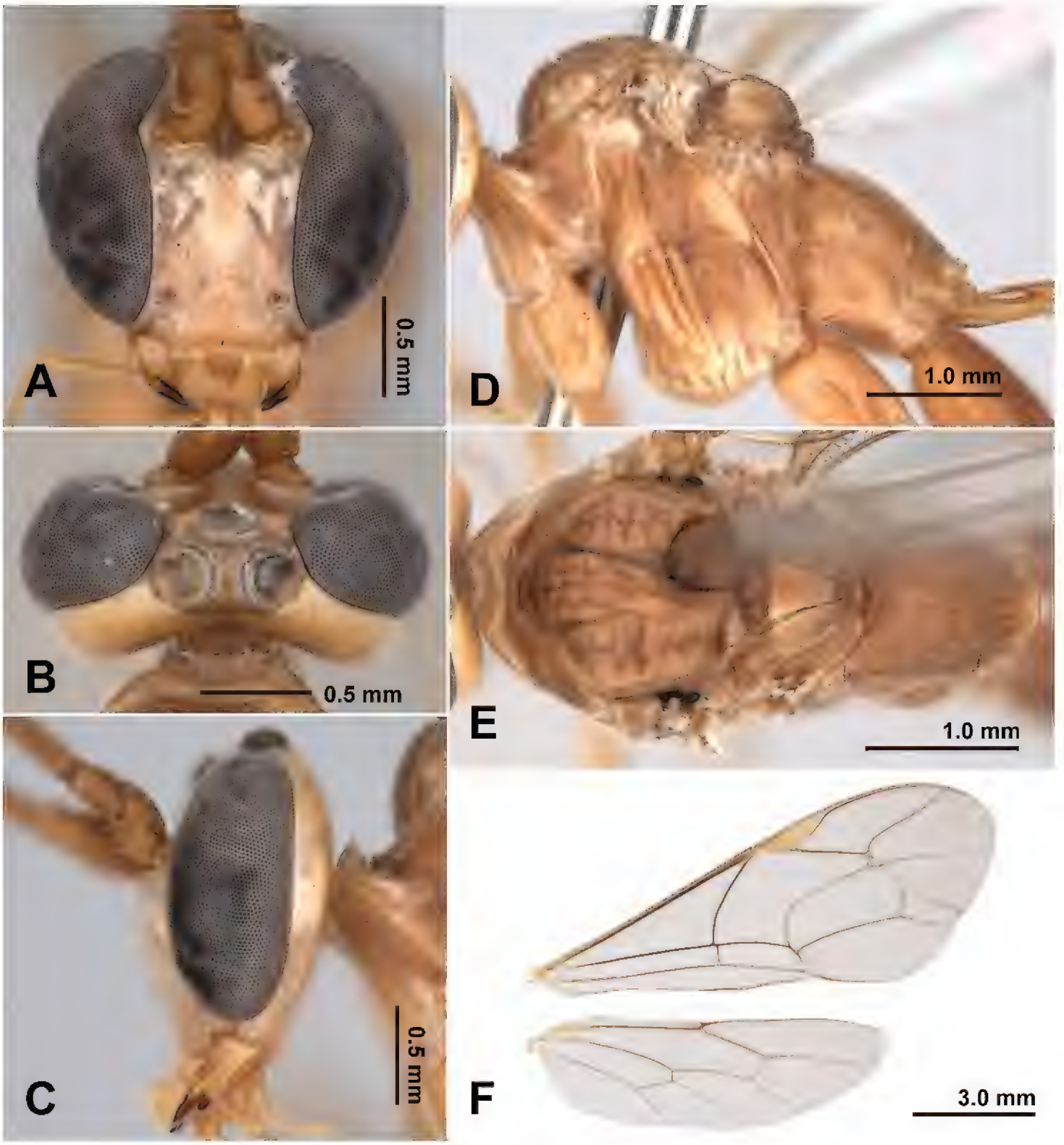

Figure 10. Taiwanese specimen of *Netelia* (*Paropheltes*) *savchenkoi* Tolkanitz, 1981 (male) **A** head in anterior view **B** head in dorsal view **C** head in lateral view **D** mesosoma in lateral view **E** mesosoma in dorsal view **F** wings. Specimen: **A–F** NMNS ENT 9068-2 (CHP01326).

NMNS ENT 8951-9. 1 ♂; Ren'ai Township, Meifeng; 15–22. V. 1979; Malaisetrap; Unknown collector; Voucher: TARI Net 2. 3 ♂♂; ibid, 15–22. XI. 1979; Voucher: TARI Net 3–5. 1 ♂; Lugu ('Luku') Township; Sitou Observatory; 20–21. IX. 2006; Mercury Light; Chan, Lan, Liang, Wu, Hung leg.; Voucher: NMNS ENT 5347-264. – **Chiayi County** • 4 ♂♂; Alishan Township, Alishan, Tai-18th Highway 82.1k, 23.496638°N, 120.784629°E; 17. VI. 2020; light trap; C.-L. Huang leg.; GenBank: PV910504–PV910507 (*COI*); Sample ID: CHP00853–854, 856–857; Voucher: NMNS ENT 8951-15, 8951-16 (CHP00853–854), KPMNH (CHP00856–857).

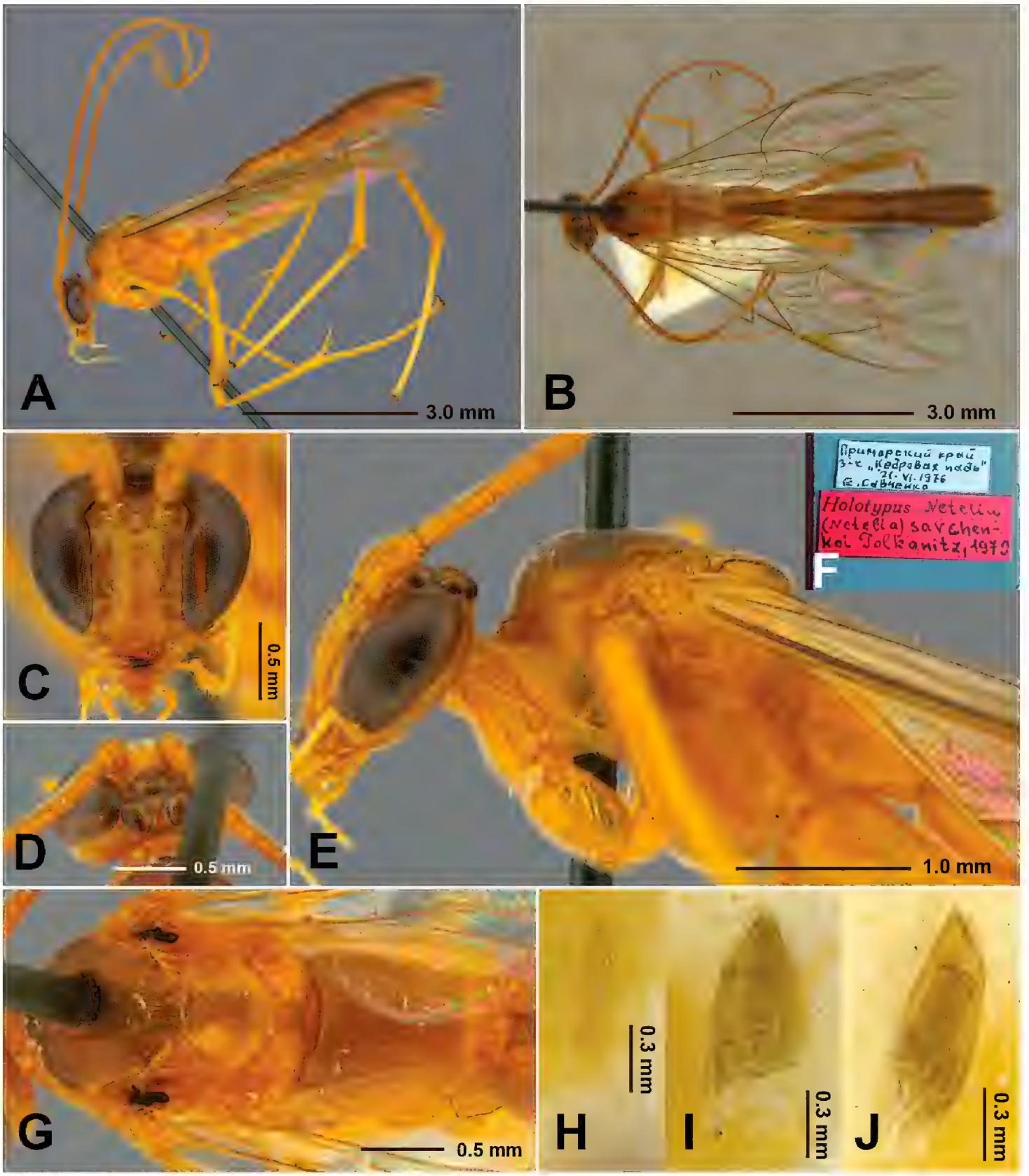

Figure 11. Holotype of *Netelia* (*Paropheltes*) *savchenkoi* Tolkanitz, 1981 (SIZU, male) **A** lateral habitus **B** dorsal habitus **C** head in anterior view **D** head in dorsal view **E** head and mesosoma in lateral view **F** labels **G** mesosoma in dorsal view **H** penisvalva **I** left gonostyle **J** right gonostyle.

Redescription based on Taiwanese specimens. Measurements were based on 6 males. **Male.** ***Head*** (Figs 9A–C): vertex and frons matt and smooth; face and clypeus polished and strongly punctate with setae; HW/HL = 1.7–2.1 (1.88 ± 0.12); lateral ocelli touching eyes, OD = 0.2–0.3 (0.30 ± 0.03) mm, POL/OD = 0.3–0.4 (0.38 ± 0.05); occipital carina present but absent dorsally; face FW/FH = 1.1–1.2 (1.11 ± 0.05); clypeus CLW/CLH = 1.8–2.1 (1.96 ± 0.08), ventral margin trun-

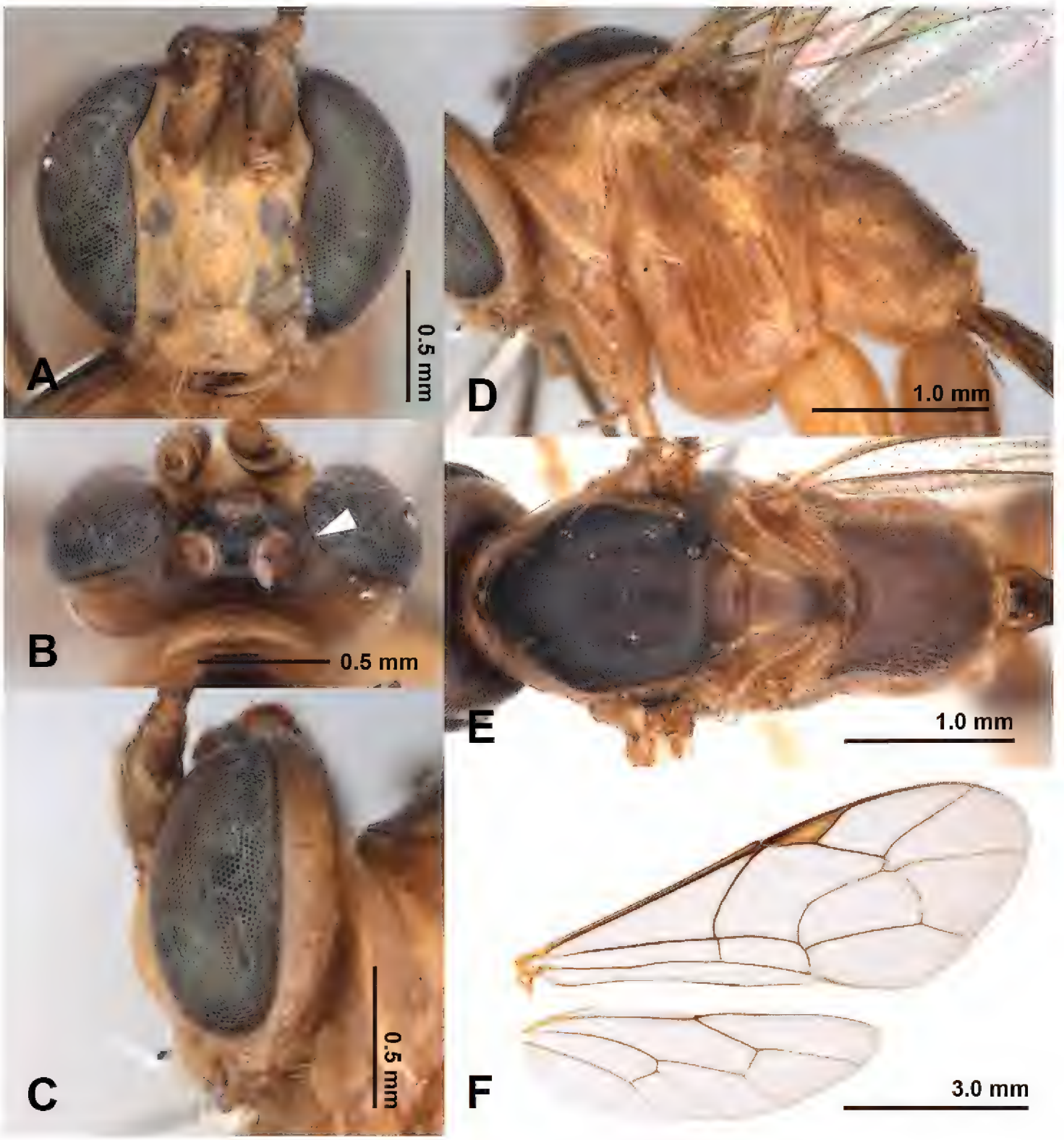

Figure 12. Taiwanese specimens of *Netelia* (*Paropheltes*) *yui* Konishi, 2000 (male) **A** head in anterior view **B** head in dorsal view, the white triangle indicates the lateral ocellus that not touching the eye **C** head in lateral view **D** mesosoma in lateral view **E** mesosoma in dorsal view **F** wings. Specimen: **A–D** NMNS ENT 4477-648; **E** NMNS ENT 4477-763; **F** TARI Net12.

cated; malar space with MSL/BMW = 0.2–0.3 (0.26 ± 0.03); gena GOI = 3.1–4.1 (3.47 ± 0.41); flagellum with 42–45 segments, 1st flagellomere 1.3–1.6 (1.36 ± 0.12) × as long as 2nd flagellomere, 3.4–5.5 (4.00 ± 0.75) × as long as wide.

Mesosoma (Figs 9D, E): pronotum polished and entirely rugose-striate; mesoscutum, scutellum, and mesopleuron polished and evenly punctate; pronotum with epomia present; mesoscutum MSSL/MSSW = 1.2–1.4 (1.29 ± 0.07), with notaulus present on about anterior 0.6; scutellum SCL/SCW = 1.4–1.7 (1.56 ± 0.11), with lateral carina present on anterior 0.3; propodeum evenly and minutely punctate on

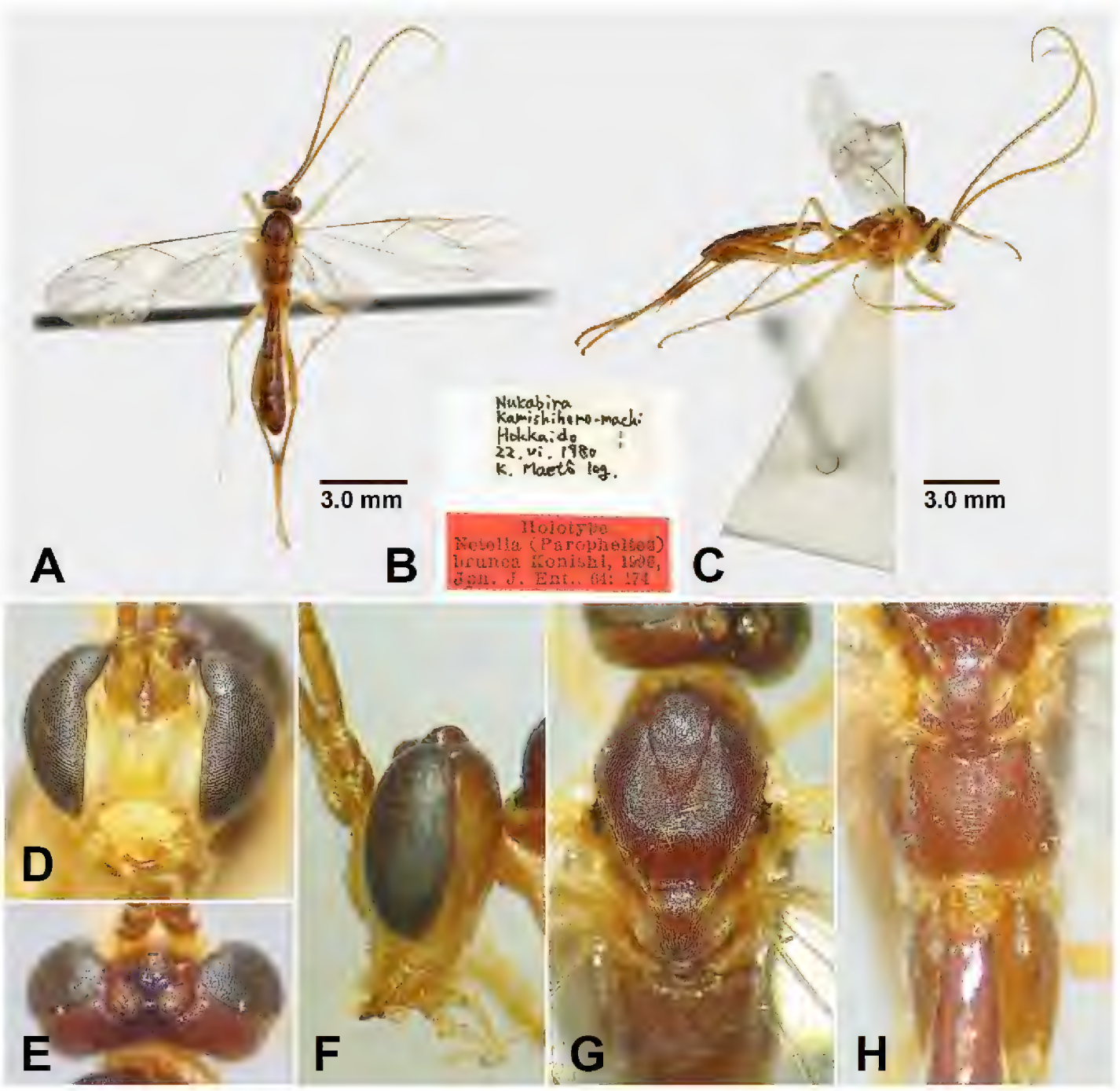

Figure 13. Holotype of *Netelia* (*Paropheltes*) *brunea* Konishi, 1996 (=*Netelia* (*Paropheltes*) *yui* Konishi, 2000) (NARO, male) **A** dorsal habitus **B** labels **C** lateral habitus **D** head in anterior view **E** head in dorsal view **F** head in lateral view **G** mesosoma and scutellum in dorsal view **H** propodeum and T1 in dorsal view.

about anterior 0.2, with strong rugose-transverse striae posteriorly, sublateral crest strong and almost connected dorsally.

Wings (Fig. 9F): fore wing length 9.4–10.7 (9.87 ± 0.46) mm; 3rs-m present, areolet medium-sized and anteriorly pointed; 2rs-m and abscissa between 2rs-m and 2m-cu in obtuse angle; RMI = 0.7–1.1 (0.86 ± 0.12); ramulus absent; 1cu-a slightly curved and vertical, far distad to M&RS with BNI = 0.7–1.0 (0.83 ± 0.14); cell AA with setal band broad and parallel-sided; AA down-curved on middle; hind wing with distal 5–6 hamuli; NI = 0.3–0.4 (0.33 ± 0.03).

***Legs*:** fore tibial spur 0.3–0.4 (±) × as long as 1st tarsomere; fore 1st tarsomere 14.3–18.8 (17.51 ± 1.81) × as long as wide, 1.6–1.7 (1.66 ± 0.04) × as long as 2nd; fore tarsal claw with 19–20 pectens; hind 1st tarsomere 12.3–14.1 (13.06 ± 0.70) × as long as wide, 1.8–2.0 (1.91 ± 0.07) × as long as 2nd; hind tarsal claw normal, with 13–15 pectens.

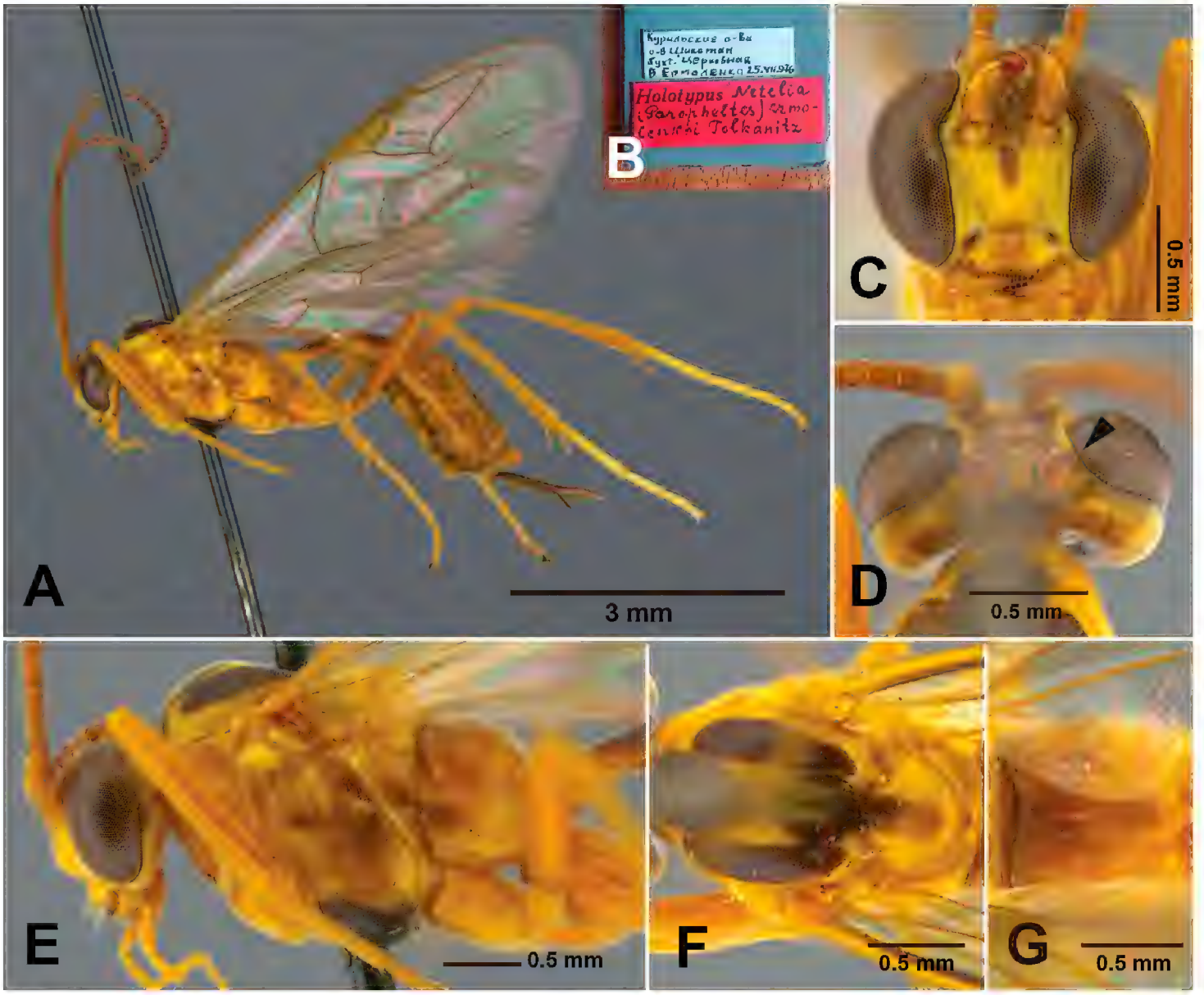

Figure 14. Holotype of *Netelia* (*Paropheltes*) *ermolenkoi* Tolkanitz, 1981 (SIZU, female) **A** lateral habitus **B** labels **C** head in anterior view **D** head in dorsal view, the black triangle indicates the lateral ocellus that almost touching the eye **E** head and mesosoma in lateral view **F** mesoscutum and scutellum **G** propodeum in dorsal view.

Metasoma (Figs 17E–G): T1 4.2–5.2 (4.69 ± 0.36) × as long as posterior width, 1.5–1.9 (1.66 ± 0.12) × as long as T2; abdominal sternum IX HPW/HPL = 0.9–1.0 (0.92 ± 0.02), posteriorly strongly convex with weak notch medially; gonostyle small and apically rounded, with submarginal spine absent, GSWB/GSL = 0.5 (0.49 ± 0.04), pad vestigial, located medially and projected dorso-basally, forming weak membranous overhang; brace shorter than half of gonostyle length apical to ventral apex of basivolsella; gonossiculus long and slender, broad apically and pointed ventrally; basivolsella with patch of sparse and short seta; penisvalva PVL/GSL = 0.5–0.6 (0.55 ± 0.04), volviceps with dorsal margin about 0.8 length of ventral margin, broad apically, valvura straight and slender.

Coloration (Figs 6B, 7): head yellowish white, except frons, middle of face, and occiput orange; mesosoma orange, except lateral margin and area between lateral and median lobes of mesoscutum, posterior 0.3 of scutellum, dorso-anterior corner of mesopleuron yellowish white; wings hyaline, with wing vein blackish brown and pterostigma yellowish brown; legs orange; metasoma orange.

Female. Taiwanese specimens not examined. Described in Kaur and Jonathan (1979).

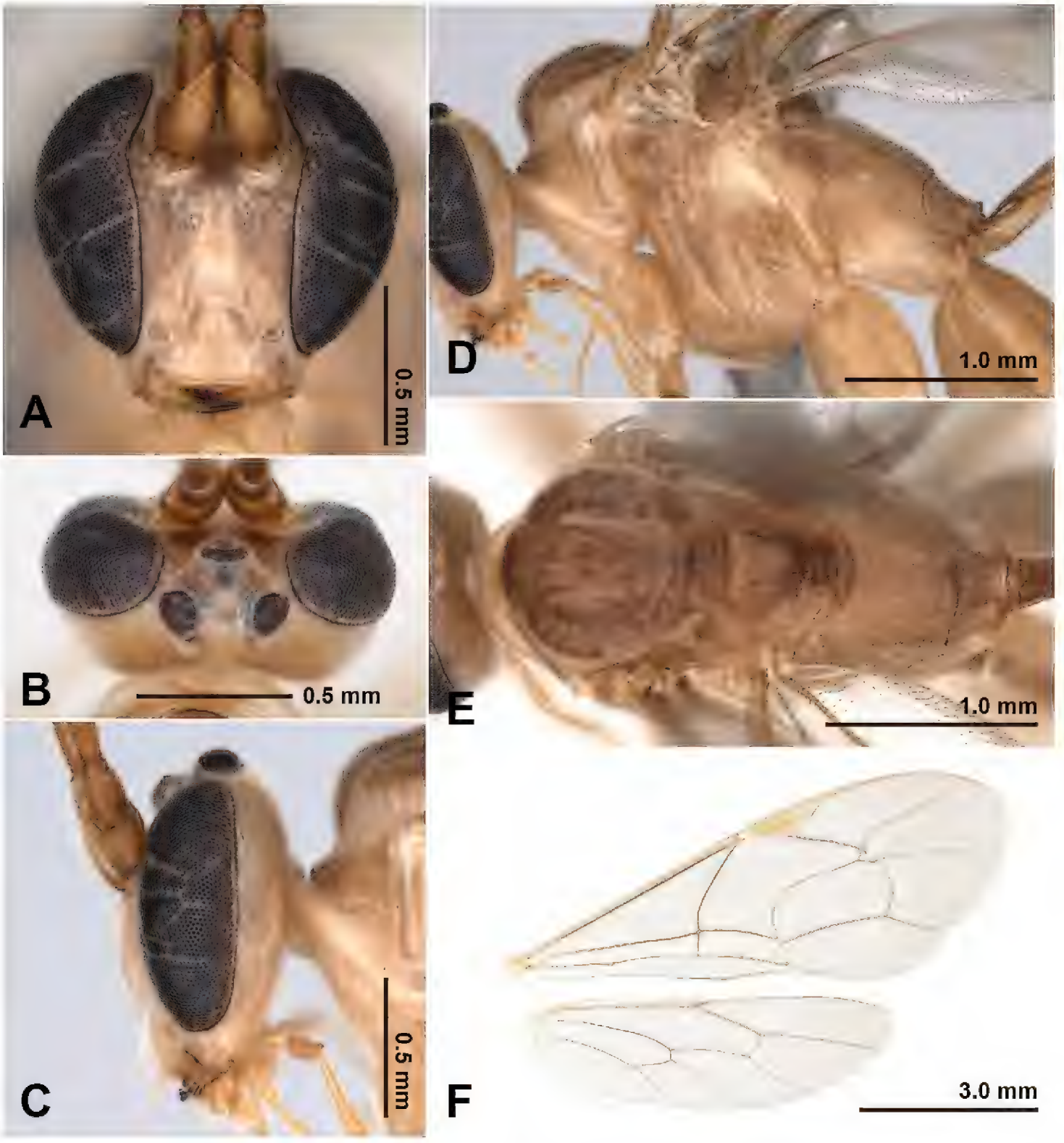

Figure 15. Holotype of *Netelia* (*Paropheltes*) *dalupalringi* Chen, Konishi & Shiao, sp. nov. (male) **A** head in anterior view **B** head in dorsal view **C** head in lateral view **D** mesosoma in lateral view **E** mesosoma in dorsal view **F** wings. Specimen: **A–F** NMNS ENT 9068-1 (CHP01409).

Distribution. India (Himachal Pradesh [type locality], Uttar Pradesh (Kaur and Jonathan 1979)), Taiwan (new record: Nantou, Chiayi).

Bionomics. Unknown.

Remarks. Although the type locality of this species, India, is far from Taiwan, the Taiwanese specimens were identified as this species based on the structure of the male genitalia and the color pattern (details as per Diagnosis section), which agree with the original description (Kaur and Jonathan 1979) without distinct variation observed. This species is the only species of *N.* (*Paro.*) *guptai* species group based on the classification of Kaur and Jonathan (1979).

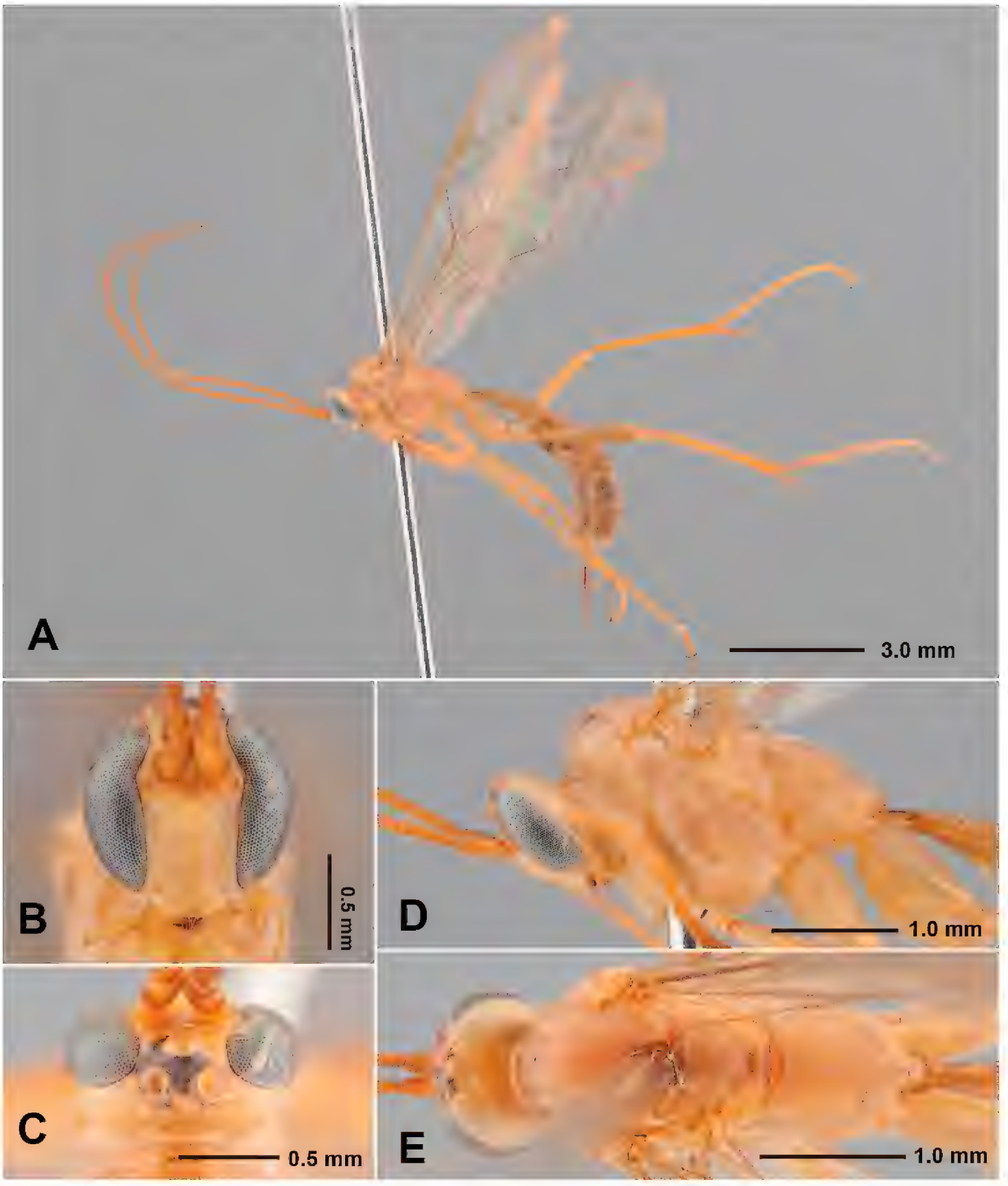

Figure 16. Female paratype of *Netelia* (*Paropheltes*) *dalupalringi* Chen, Konishi & Shiao, sp. nov. **A** lateral habitus **B** head in anterior view **C** head in dorsal view **D** mesosoma in lateral view **E** mesosoma in dorsal view. Specimen: **A–E** NMNS ENT 7423-1567.

Netelia (*Paropheltes*) *savchenkoi* Tolkanitz, 1981

Figs 6C, 10, 11, 17H–K

Netelia (*Netelia*) *savchenkoi* Tolkanitz, 1981b: 35.
Netelia (*Paropheltes*) *savchenkoi* – Konishi 1996a: 183.

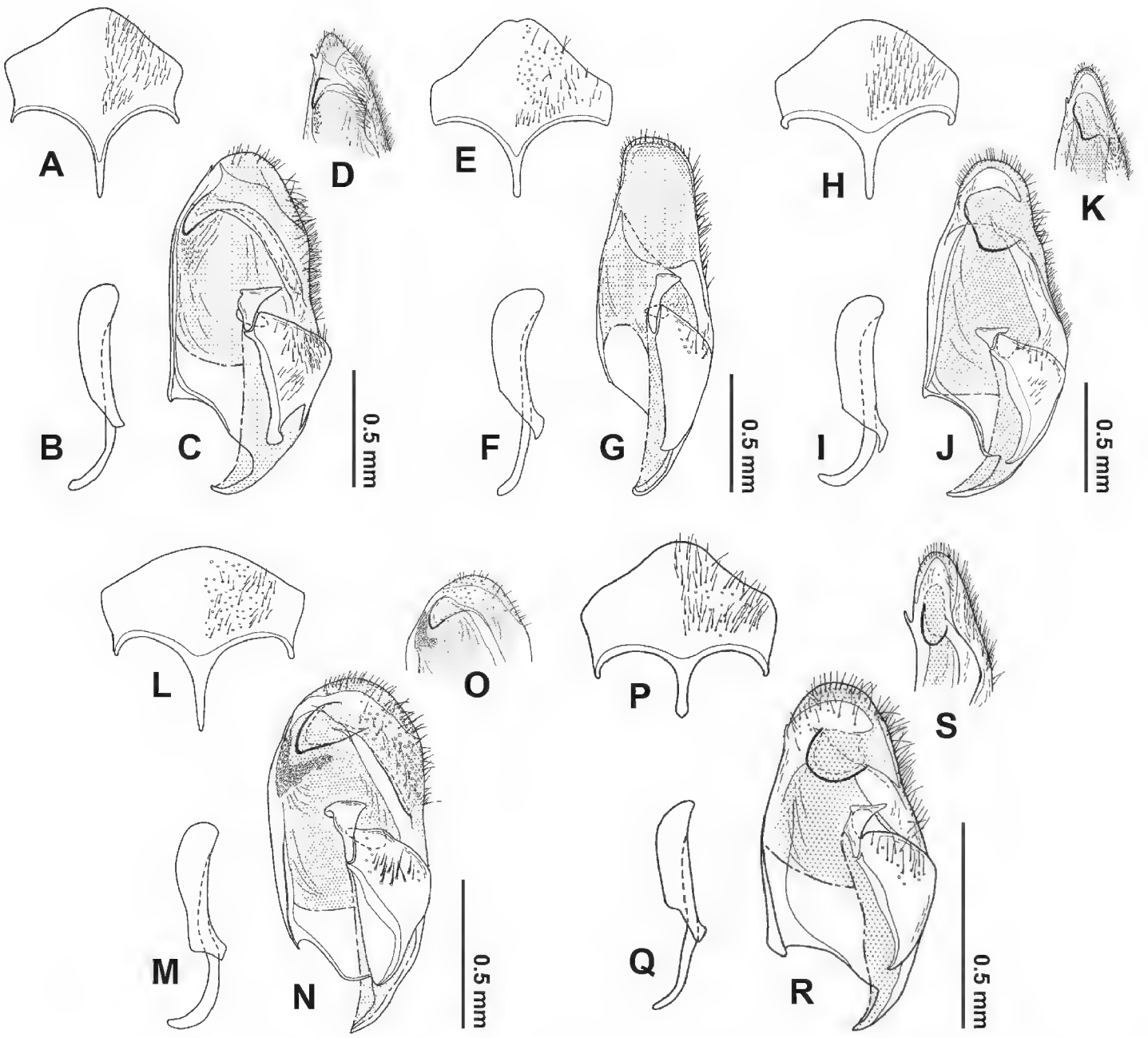

Figure 17. Male genitalia of Taiwanese species of the subgenus *Paropheltes* in the genus *Netelia* **A–D** *N.* (*Paro.*) *fulginosa* Konishi, 1996 **E–G** *N.* (*Paro.*) *guptai* Kaur & Jonathan, 1979 **H–K** *N.* (*Paro.*) *savchenkoi* Tolkanitz, 1981 **L–O** *N.* (*Paro.*) *yui* Konishi, 2000 **P–S** *N.* (*Paro.*) *dalupalringi* Chen, Konishi & Shiao, sp. nov. **A, E, H, L, P** abdominal sternum IX **B, F, I, M, Q** penisvalva **C, G, J, N, R** gonostyles in inner view **D, K, S** apical gonostyles in ventral view **O** variation of the papillate area in the inner view of the gonostyles. Illustrated by HPC.

Diagnosis. This species can be distinguished from other species of subgenus *Paropheltes* in having the combination of the following characters: occipital carina complete in most specimens, absent dorsally in some specimens; scutellum with lateral carina present on anterior 0.8 to 0.9; gonostyle with submarginal spine present; pad rounded rectangular and projected dorso-basally, connected with conjunctiva ventro-apically; brace broadened basally and narrow apically.

Type material. ***Holotype.*** Russia • 1 ♂; "Приморский край, Кедровая падь" [Primorsky Krai, Kedrovaya Pad]; 21. VI. 1976; "Савченко" [Savchenko] leg.; light trap; Voucher: SIZU (Fig. 11).

Non-type material. Taiwan – **Nantou County** • 1 ♂; Xingyi Township, Tatajia, Tai-18th highway 100.5 k, 23.480555°N, 120.852519°E; 16. VI. 2020; light trap;

C.-L. Huang leg.; GenBank: PV910511 (*COI*); Sample ID: CHP01326; Voucher: NMNS ENT 9068-2. 1 ♂; Ren'ai Township, Meifeng; 24. IV. 1991; UV light trap; C. S. Sun leg.; Voucher: NMNS ENT 818-21. 3 ♂♂; ibid, Tayuling, 820 forest road (Fogeste); UV light trap; 3. IX. 2008; H.H. Lin leg.; Voucher: NMNS ENT 6070-580, 1199–1200. 2 ♂♂; ibid, Tsuifeng; alt. 2300 m; Malaise trap; X. 1985; K. S. Lin leg.; Voucher: TARI Net 32, 41. – **Hualien County** • 1 ♂; Xiulin [Hsiulin] Township; Kuan-yun Hostel; alt. 2335 m; 27–28. V. 2008; UV light trap; Liang, Chen, Fu leg.; Voucher: NMNS ENT 5921-1017. – **Chiayi County** • 1 ♂; Alishan Township, Alishan, 23.47666°N, 120.71583°E; 28. IV. 2023; light trap; C.-Y. Juang leg.; GenBank: PV910510 (*COI*); Sample ID: CHP01278; Voucher: TARI.

Redescription based on Taiwanese specimens. Measurements were based on 9 males. **Male.** ***Head*** (Figs 10A–C, 11C–E): vertex matt, weakly and finely coriaceous; frons, face and clypeus matt and coriaceous with setae; HW/HL = 1.6–2.2 (1.9 ± 0.18), lateral ocelli almost touching eyes, OD = 0.2–0.3 (0.26 ± 0.01) mm, POL/OD = 0.3–0.5 (0.38 ± 0.06); occipital carina complete, sometimes absent dorsally; face FW/FH = 1.0–1.2 (1.09 ± 0.06); clypeus CLW/CLH = 2.0–2.4 (2.17 ± 0.13), ventral margin weakly concave; malar space with MSL/BMW = 0.2–0.6 (0.33 ± 0.10); gena GOI = 2.8–4.0 (3.36 ± 0.43); flagellum with 45–48 segments, 1st flagellomere 1.2–1.4 (1.27 ± 0.09) × as long as 2nd flagellomere, 3.9–5.8 (4.58 ± 0.57) × as long as wide.

Mesosoma (Figs 10D, E, 11E, F): pronotum polished, minutely punctate dorsally and rugose medially; mesoscutum and scutellum matt, evenly and minutely punctate; mesopleuron polished and minutely punctate; mesoscutum MSSL/MSSW = 1.1–1.4 (1.27 ± 0.08), with notaulus present on about anterior 0.4; scutellum SCL/SCW = 1.1–1.7 (1.42 ± 0.19), with lateral carina present on anterior 0.8 to 0.9; propodeum evenly and minutely punctate on anterior half, with dense and transverse striae posteriorly, sublateral crest normal, not connected dorsally.

Wings (Figs 10F, 11B): fore wing length 8.5–10.2 (9.42 ± 0.60) mm; 3rs-m present, areolet medium-sized and anteriorly stalked; 2rs-m and abscissa between 2rs-m and 2m-cu in acute angle; RMI = 0.8–1.5 (1.04 ± 0.20); ramulus absent; 1cu-a straight and vertical, distad to M&RS with BNI = 0.1–0.4 (0.24 ± 0.08); cell AA with setal band narrow and sparse on about proximal 0.3–0.5; AA almost straight; hind wing with distal 6–7 hamuli; NI = 0.3–0.4 (0.33 ± 0.05).

***Legs*:** fore tibial spur 0.3–0.4 (0.31 ± 0.06) × as long as 1st tarsomere; fore 1st tarsomere 14.0–19.3 (17.36 ± 1.72) × as long as wide, 1.7–1.9 (1.77 ± 0.08) × as long as 2nd; fore tarsal claw with 16–19 pectens; hind 1st tarsomere 11.3–16.1 (14.24 ± 1.53) × as long as wide, 1.8–2.1 (1.97 ± 0.11) × as long as 2nd; hind tarsal claw normal, with 12–15 pectens.

Metasoma (Figs 17H–K, 11H–J): T1 4.0–5.2 (4.41 ± 0.41) × as long as posterior width, 1.4–1.7 (1.56 ± 0.09) × as long as T2; abdominal sternum IX HPW/HPL = 0.8–1.1 (0.99 ± 0.09), posteriorly rounded; gonostyle rounded and weakly tapered apically, with submarginal spine present on about dorso-apical 0.2, GSWA/GSL = 0.3 (0.31 ± 0.02), GSWB/GSL = 0.5–0.6 (0.56 ± 0.05), GSWB/GSWA = 1.7–1.9 (1.83 ± 0.05), pad rounded rectangular and projected dorso-basally, connected with conjunctiva ventro-apically; brace broad basally and narrow apically; gonossiculus

short, broad apically and pointed ventrally; basivolsella with patch of sparse and short seta; penisvalva PVL/GSL = 0.5–0.7 (0.58 ± 0.04), volviceps with dorsal margin about 0.9 length of ventral margin, valvura strongly and dorsally curved.

Coloration (Figs 6C, 10, 11): head yellowish brown, except face yellowish white and dorsal portion of occiput sometimes brown; mesosoma yellowish brown, with mesoscutum and dorsal surface of propodeum brown, speculum and anterior corner of mesopleuron yellowish white; wings hyaline, with wing vein yellowish brown and pterostigma pale yellowish brown; legs yellowish brown, except hind coxa brown, hind tarsus yellowish white to yellow; metasoma yellowish brown.

Female. Taiwanese specimens not examined. Described in Tolkanitz (1981b) and Konishi (1996a).

Distribution. Russia (Promorskii Krai [type locality] (Tolkanitz 1981b)), Japan (Honshu, Shikoku, Kyushu (Konishi 1996a)), Taiwan (new record: Nantou, Hualien, Chiayi).

Bionomics. This species was collected from the mountains between the elevation 1320–2400 m in Taiwan. This new record extends the distribution of an eastern Palearctic species to the mountain areas of a subtropical region.

Remarks. Despite minor variations in general morphology and male genitalia observed between the Taiwanese and eastern Palearctic specimens, these differences are considered intraspecific variation. For instance, the lateral carina extends beyond the anterior 0.8 in Russian and Taiwanese specimens but only reaches 0.8 in Japanese specimens (Konishi 1996a), and the brace is narrower in Taiwanese specimens but broader in Japanese and Russian specimens (Tolkanitz 1981b; Konishi 1996a).

This species can be assigned to the *N.* (*Paro.*) *barberi* species group based on the brownish mesosoma without any distinctive yellow marking and lateral carina of scutellum extending beyond 0.7 of its length.

Netelia (*Paropheltes*) *yui* Konishi, 2000

Figs 6D–E, 12, 13, 17L–O

Netelia (*Paropheltes*) *brunea* Konishi, 1996a: 174. Preoccupied by *Netelia* (*Netelia*) *brunnea* Townes, 1939.

Netelia (*Paropheltes*) *yui* Konishi, 2000: 290. Substitute name of *Netelia* (*Paropheltes*) *brunea* Konishi, 1996.

Diagnosis. This species can be distinguished from other species of subgenus *Paropheltes* in having the combination of the following characters: occipital carina complete; gonostyle with a papillate area (V-shaped or weakly present dorsally) on apex of the pad; gonostyle with submarginal spine absent; mesopleuron yellowish brown, brown, to blackish brown; mesoscutum completely blackish brown.

This species is most similar to *N.* (*Longiterebates*) *turgida* Kaur & Jonathan, 1979 and *N.* (*Paro.*) *ermolenkoi* Tolkanitz, 1981 in having the rounded and blunt gonostyle, narrow and parallel-sided brace, apically pointed and dorso-basally projected pad, presence of

papillate area dorsally, but differs in the complete occipital carina (absent in *N.* (*Longiterebates*) *turgida*) (Konishi, 1996a), the almost completely brown or blackish brown mesoscutum (Figs 12E, 13G) (three brownish stripes on lobes of mesoscutum in *N.* (*Paro.*) *ermolenkoi* (Fig. 14F)), the mesopleuron with brownish markings and mesosternum without blackish brown markings (Figs 12D, 13C) (pale yellowish brown mesopleuron with blackish brown mesosternum in *N.* (*Paro.*) *ermolenkoi* (Fig. 14E)), the fore wing 1cu-a almost opposite or slightly distad to M&RS (Figs 12F, 13A) (basad to M&RS in *N.* (*Paro.*) *ermolenkoi* (Fig. 14A)), and the lateral ocelli not touching eyes (Fig. 12B) (almost touching eyes in *N.* (*Longiterebates*) *turgida* and *N.* (*Paro.*) *ermolenkoi* (Fig. 14D)).

Type material. ***Holotype.*** Japan • 1 ♂; Hokkaido, Tokachi, Kamishihoro-machi, Nukabira; 22. VI. 1980; K. Maeto leg.; Voucher: NARO (Fig. 13).

Non-type material. Taiwan – **Hualien County** • 1 ♂; Xiulin Township, Tayuling; alt. 2560 m; 9–16. VI. 1980; K. S. Lin, B. H. Chen leg.; Voucher: TARI Net 6. – **Taichung City** • 1 ♀; Heping Dist., Anmashan; alt. 2275 m; 6–9. VII. 1979; L. Y. Chou leg.; Voucher: TARI Net 7. 1 ♀; ibid, Wuling; alt. 1900 m; 27–29. VI. 1979; K. S. Lin, L. Y. Chou leg.; Voucher: TARI Net 8. – **Nantou County** • 3 ♂♂; Ren'ai Township, Meifeng; 11. VI.–9. VII. 2002; Malaise trap (KCN); C. S. Lin, W. T. Yang leg.; Voucher: NMNS ENT 4477-571, 648, 763. 1 ♂; ibid; alt. 2150 m; 20–22. VI. 1979; K. S. Lin, B. S. Chen leg.; Voucher: TARI Net 9. 1 ♂; ibid; 5–8. VI. 1980; C. C. Chen leg.; Voucher: TARI Net 10. 1 ♀; Ren'ai Township, Peitungyanshan; 1–31. X. 1972; Malaise trap; Unknown collector; Voucher: TARI Net 11. 3 ♀♀; Ren'ai Township, Sungkang; alt. 2100 m; X. 1985; Malaise trap; K. S. Lin leg.; Voucher: TARI Net 23–25. – **Chiayi County** • 1 ♂; Alishan Township, Alishan; alt. 2400 m; 5–9. VIII. 1981; L. Y. Chou, S. C. Lin leg.; Voucher: TARI Net 12. Japan – **Kanagawa Prefecture** • 1 ♂; Yamakita, Mt. Hinokiboramaru; 17. VII. 2014; T. Taniwaki leg.; Voucher: KPMNH. **Shizuoka Prefecture** • 1 ♂; Shizuoka City, Aoi-ku, Kangyoumine-toge; 14. VI. 2008; K. Watanabe leg.; Voucher: KPMNH.

Redescription based on Taiwanese specimens. Measurements were based on 6 males and 3 females. **Male.** ***Head*** (Figs 12A–C, 13D–F): vertex polished and coriaceous; frons, face, clypeus matt and finely coriaceous with setae; HW/HL = 1.79–2.11(1.94 ± 0.13),; lateral ocelli not touching eyes, OD = 0.2 (0.20 ± 0.02) mm, POL/OD = 0.3–0.6 (0.44 ± 0.09), minimum distance between eye and lateral ocelli/OD = 0.2–0.3 (0.28 ± 0.05); occipital carina complete; face FW/FH = 1.3–1.4 (1.30 ± 0.04); clypeus CLW/CLH = 1.8–2.4 (2.20 ± 0.25), ventral margin truncated; malar space with MSL/BMW = 0.2–0.4 (0.34 ± 0.08); gena GOI = 2.2–2.9 (2.67 ± 0.26); flagellum with 39–41 segments, 1st flagellomere 1.2–1.4 (1.28 ± 0.08) × as long as 2nd flagellomere, 4.0–5.0 (4.50 ± 0.36) × as long as wide.

Mesosoma (Figs 12D, E; 13G, H): pronotum matt and coriaceous, rugose on middle area; mesoscutum, scutellum, and mesopleuron matt, normally or finely coriaceous; mesoscutum MSSL/MSSW = 1.2–1.4 (1.27 ± 0.09), with notaulus present on about anterior 0.4; scutellum SCL/SCW = 1.1–1.5 (1.20 ± 0.16), with lateral carina present on about anterior 0.3; propodeum evenly and minutely punctate on anterior half, with strong and parallel transverse striae posteriorly, sublateral crest absent or weak.

Wings (Figs 12F, 13A): fore wing length 6.2–7.2 (6.73 ± 0.43) mm; 3rs-m present, areolet medium-sized and anteriorly stalked; 2rs-m and abscissa between 2rs-m and 2m-cu in acute angle; RMI = 0.8 (0.80 ± 0.03); ramulus absent; 1cu-a straight and weakly inclivous, basad to M&RS with BNI = 0.1–0.2 (0.16 ± 0.03); cell AA with setal band sparse and parallel-sided; AA almost straight; hind wing with 6 distal hamuli; NI = 0.2–0.4 (0.37 ± 0.08).

***Legs*:** fore tibial spur 0.3–0.4 (0.33 ± 0.02) × as long as 1st tarsomere; fore 1st tarsomere 16.0–19.5 (17.71 ± 1.51) × as long as wide, 2.0–2.1 (2.04 ± 0.06) × as long as 2nd; fore tarsal claw with 8–9 pectens; hind 1st tarsomere 10.5–12.9 (11.48 ± 0.96) × as long as wide, 2.0–2.2 (2.06 ± 0.06) × as long as 2nd; hind tarsal claw normal, with 6 pectens.

Metasoma (Fig. 17L–O): T1 3.1–3.6 (3.42 ± 0.18) × as long as posterior width, 1.6–1.7 (1.60 ± 0.05) × as long as T2; abdominal sternum IX HPW/HPL = 0.9–1.1 (1.02 ± 0.09), posteriorly rounded; gonostyle apically rounded and blunt, with submarginal spine absent, GSWB/GSL = 0.5–0.6 (0.59 ± 0.04), pad apically pointed, projected dorso-basally; brace narrow and parallel-sided; papillate area V-shaped (not well developed in some specimens) on apex of pad; gonossiculus narrow, strongly broad apically and pointed ventrally; basivolsella with patch of long and stout seta; penisvalva PVL/GSL = 0.5–0.6 (0.54 ± 0.05), volviceps with dorsal margin about 0.9 length of ventral margin, valvura strongly and dorsally curved.

Coloration (Figs 6D, E, 12, 13A, B): head yellowish brown, except ocellar area blackish brown, vertex and dorsal portion of occiput brown; mesosoma yellowish brown except mesoscutum blackish brown, apical 0.3 of scutellum and dorsal surface of propodeum brown; wings hyaline, with wing vein blackish brown and pterostigma brown to yellowish brown; legs yellowish brown, except fore and mid tarsi, hind femora and tibia brown, hind tarsi yellowish white; metasoma yellowish brown to brown.

Female. General structures and color similar to male. HW/HL = 1.9–2.2 (2.06 ± 0.16); OD = 0.2 (0.20 ± 0.02) mm, POL/OD = 0.4–0.6 (0.48 ± 0.07), minimum distance between eye and lateral ocelli/OD = 0.2–0.3 (0.26 ± 0.07); FW/FH = 1.2–1.3 (1.23 ± 0.06); CLW/CLH = 2.0–2.4 (2.18 ± 0.20); MSL/BMW = 0.3–0.5 (0.36 ± 0.09); GOI = 2.5–3.1 (2.76 ± 0.34); flagellum with 41–43 segments, 1st flagellomere 1.1–1.3 (1.16 ± 0.12) × as long as 2nd flagellomere, 4.0–4.8 (4.33 ± 0.43) × as long as wide. MSSL/MSSW = 1.2–1.3 (1.22 ± 0.05); SCL/SCW = 1.2–1.5 (1.38 ± 0.13); fore wing length 6.2–8.8 (7.35 ± 1.03) mm; RMI = 0.7–1.0 (0.80 ± 0.14); BNI = 0.2 (0.21 ± 0.03); hind wing with 6 hamuli; NI = 0.3 (0.29 ± 0.03). Fore tibial spur 0.3–0.4 (0.35 ± 0.05) × as long as 1st tarsomere; fore 1st tarsomere 15.5–20.1 (17.44 ± 2.42) × as long as wide, 2.0–2.2 (2.08 ± 0.11) × as long as 2nd; fore tarsal claw with 6 pectens; hind 1st tarsomere 9.1–16.7 (12.22 ± 3.99) × as long as wide, 1.8–2.2 (1.98 ± 0.21) × as long as 2nd; hind tarsal claw with 6–7 pectens. T1 3.0–3.3 (3.19 ± 0.18) × as long as posterior width, 1.5–1.7 (1.59 ± 0.06) × as long as T2; ovipositor 2.1–2.4 (2.29 ± 0.14) × as long as apical depth of metasoma.

Distribution. Japan (Hokkaido [type locality], Honshu (Konishi, 1996a)), Taiwan (new record: Hualien, Taichung, Nantou, Chiayi).

Bionomics. Unknown.

Remarks. This species cannot be assigned to any known species groups of subgenus *Paropheltes*. A large color variation between the Taiwanese and Japanese specimens was observed, for instance, the mesopleuron is yellowish brown in Taiwanese specimens but with brown to blackish brown marking in Japanese specimens, and the frons is yellowish brown to brown in Taiwanese specimens but with distinct triangular brown marking in Japanese specimens.

In addition, the close distribution (Hokkaido vs. Kuril Islands and Primorsky Krai) and similar male genitalia of *N. yui* Konishi, 2000 and *N. ermolenkoi* Tolkanitz, 1981 (Tolkanitz 1999: 634, fig. 1) raising the possibility that *N. yui* could be a junior synonym of *N. ermolenkoi*. However, the structural distinctions in ocelli, fore wing vein, and body color pattern noted in the Diagnosis section above (Fig. 14), along with the possibility that the male specimens and female holotype of *N. ermolenkoi* may be mismatched (e.g., Kaur and Jonathan (1979) misidentified and incorrectly matched the male with *N.* (*Apatagium*) *inaequalis* (Uchida, 1934), a species known only from the female holotype), lead us to retain their status as separate species. Further studies, including broader sampling and DNA barcoding comparisons, are needed to clarify their taxonomic relationship.

The male genitalia of the holotype of *N.* (*Paro.*) *brunea* Konishi, 1996a (=*N.* (*Paro.*) *yui* Konishi, 2000) were observed to be missing upon personal examination by the first author in 2023. It is possible that the male genitalia may have been corroded by potassium hydroxide during the preservation process of the specimen. However, the male genitalia and other morphology (e.g., complete occipital carina, lateral ocelli distanced from eyes) of the Taiwanese specimens align with the original description (Konishi, 1996a). The Taiwanese specimens is thus considered to belong to this species.

***Netelia* (*Paropheltes*) *dalupalringi* Chen, Konishi & Shiao, sp. nov.**

https://zoobank.org/BFB160BF-3E94-43B1-97F9-5538277BCBAB

Figs 6F, 15, 16, 17P–S

Diagnosis. This species can be distinguished from other species of subgenus *Paropheltes* in having the combination of the following characters: occipital carina vestigial dorsally or completely absent; scutellum with lateral carina extend to about 0.6 of its length; propodeum with sublateral crest strong; gonostyle parallel-sided and rounded blunt apically, with submarginal spine present; pad semi-circular and projected dorso-basally; brace parallel-sided basally and narrow apically; penisvalva with valvura long and slender.

This species resembles *Netelia* (*Paropheltes*) *caucasica* (Kokujev, 1899) in the general shape of the gonostyle and pad, as described in the original description and by Konishi (1996a). However, it differs in having a parallel-sided gonostyle (tapered in *N.* (*Paro.*) *caucasica*), a submarginal spine presents subapically on the dorsal gonostyle (absent in *N.* (*Paro.*) *caucasica*), and a pale yellowish-brown mesosoma (dark brown to black mesosoma in *N.* (*Paro.*) *caucasica*).

Type material. ***Holotype.*** Taiwan – **Kaohsiung City** • 1 ♂; Maolin Dist., Lake Dalupalringi, 22.86852°N, 120.85906°E; alt. 2180 m; 26. I. 2024; light trap; Y. Yang & I.-L. Lee leg.; GenBank: PV910502 (*COI*); Sample ID: CHP01409; Voucher: NMNS ENT 9068-1. ***Paratypes.*** Taiwan – **Nantou County** • 1 ♂; Ren'ai Township, Yuanfeng; 7. VIII.–11. IX. 2001; Malaise trap; C. S. Lin, W. T. Yang leg.; Voucher: NMNS ENT 4229-109. 1 ♂; ibid; 15. X.–12. XI. 2002; Voucher: NMNS ENT 4374-345. 2 ♂♂; ibid; alt. 2756 m; 7. X.–4. XI. 2003; Voucher: NMNS ENT 6658-413–414. 2 ♂♂; ibid; 21. IX. –17. X. 2006; Voucher: NMNS ENT 7470-230, 233. 1 ♂; ibid; 14. VII. –7. VIII. 2007; Voucher: NMNS ENT 7825-1363. 3 ♀♀; ibid; 7. VI.–5. VII. 2005; Voucher: NMNS ENT 7392-416–418. 3 ♀♀; ibid; 11. VI.–8. VII. 2003; Voucher: NMNS ENT 6626-541, 546–547. 1 ♀; ibid; 8. VII.–5. VIII. 2003; Voucher: NMNS ENT 6626-1217. 6 ♀♀; ibid; 6. VI.–25. VII. 2006; Voucher: NMNS ENT 7423-1566–1567, 1569–1571, 1574. 1 ♂; Ren'ai Township, Meifeng; alt. 2150 m; XI. 1985; K. S. Lin leg.; Voucher: TARI Net 28. 1 ♂; ibid; 7–9. V. 1981; K.S. Lin, S. C. Lin leg.; Voucher: TARI Net 37. 2 ♂♂; Ren'ai Township, Sungkang; alt. 2100 m; X. 1985; Malaise trap; K. S. Lin leg.; Voucher: TARI Net 26–27. 1 ♂; ibid; XI. 1985; Voucher: TARI Net 45. 1 ♂; Ren'ai Township, Tsuifeng; alt. 2300 m; X. 1985; Malaise trap; K. S. Lin leg.; Voucher: TARI Net 36, 41; 5 ♂♂; ibid; XI. 1985; Voucher: TARI Net 34–35, 38–40. 1 ♂; ibid; alt. 2300–2500 m; 21. VI. 1979; K. S. Lin, B. H. Chen leg.; Voucher: TARI Net 42. **Hualien County** • 1 ♀; Xiulin Township, Tayuling; alt. 2560 m; 12–15. IX. 1980; K.S. Lin, C.H. Wang leg.

Description. Measurements were based on 19 males and 6 females, including the holotype. **Male.** ***Head*** (Fig. 15A–C): vertex polished and finely coriaceous; frons, face, and clypeus matt and finely coriaceous with setae; HW/HL = 1.7–2.1 (1.84 ± 0.14) [2.0], lateral ocelli almost touching eyes or not in some specimens, OD = 0.2–0.3 (0.20 ± 0.02) [0.2] mm, POL/OD = 0.4–0.8 (0.56 ± 0.11) [0.7]; occipital carina vestigial dorsally in most specimens, sometimes completely absent; face FW/FH = 1.0–1.2 (1.05 ± 0.06) [1.1]; clypeus CLW/CLH = 1.3–2.3 (1.92 ± 0.23) [2.0], ventral margin truncated; malar space with MSL/BMW = 0.3–0.5 (0.37 ± 0.06) [0.4]; GOI = 1.9–2.8 (2.37 ± 0.22) [1.9]; flagellum with 37–41 [39] segments, 1st flagellomere 1.1–1.5 (1.35 ± 0.11) [1.3] × as long as 2nd flagellomere, 3.9–5.7 (4.86 ± 0.44) [4.6] × as long as wide.

Mesosoma (Fig. 15D, E): pronotum matt, finely coriaceous with weak striae on middle area; mesoscutum matt, evenly and minutely punctate on anterior 0.6 and finely coriaceous posteriorly; scutellum matt and finely coriaceous; mesoscutum MSSL/MSSW = 1.1–1.4 (1.22 ± 0.08) [1.1], with notaulus present on anterior 0.4; scutellum SCL/SCW = 1.1–1.7 (1.35 ± 0.16) [1.3], with lateral carina present on about anterior 0.6; mesopleuron matt and coriaceous, strongly punctate on speculum; propodeum evenly and minutely punctate on anterior half, with weak transverse striae posteriorly, sublateral crest strong and dorsally extended, (almost) connected dorsally.

Wings (Fig. 15F): fore wing length 7.4–9.6 (8.54 ± 0.53) [8.5 mm] mm; 3rs-m present, areolet large and anteriorly stalked; 2rs-m and abscissa between 2rs-m and 2m-cu in acute angle; RMI = 0.6–1.0 (0.80 ± 0.09) [0.8]; ramulus absent; 1cu-a weakly curved, almost vertical, slightly basad, distad (rarely), or almost opposite to M&RS

with BNI = 0.1–0.2 (0.13 ± 0.04) [0.1]; cell AA with setal band broad and parallel-sided; AA weakly down-curved on middle; hind wing with distal 4–6 [5] hamuli; NI = 0.2–0.5 (0.32 ± 0.07) [0.3].

***Legs*:** fore tibial spur 0.3–0.4 (0.35 ± 0.03) [0.4] × as long as 1st tarsomere; fore 1st tarsomere 12.2–19.3 (15.72 ± 1.6) [14.8] × as long as wide, 1.7–1.9 (1.80 ± 0.06) [1.8] × as long as 2nd; fore tarsal claw with 18–26 [23] pectens; hind 1st tarsomere 11.4–15.8 (13.65 ± 1.41) [14.5] × as long as wide, 1.9–2.1 (2.00 ± 0.08) [1.9] × as long as 2nd; hind tarsal claw normal, with 13–19 pectens.

Metasoma (Fig. 17P–S): T1 2.4–5.1 (4.15 ± 0.55) [3.9] × as long as posterior width, 1.5–1.9 (1.64 ± 0.10) [1.6] × as long as T2; abdominal sternum IX HPW/HPL = 1.0–1.2 (1.09 ± 0.11) [1.1], posteriorly convex; gonostyle parallel-sided and rounded blunt apically, with submarginal spine present dorso-apically, GSWA/GSL = 0.3–0.4 (0.39 ± 0.02) [0.4], GSWB/GSL = 0.5–0.7 (0.58 ± 0.04) [0.6], GSWB/GSWA = 1.3–1.6 (1.48 ± 0.09) [1.5], pad semi-circular, located medially and projected dorso-basally, connected with conjunctiva ventro-apically; brace parallel-sided basally and narrow apically; gonossiculus long, broad apically and pointed ventrally; basivolsella with patch of medium to long seta; penisvalva PVL/GSL = 0.5–0.6 (0.53 ± 0.03) [0.5], volviceps slender, with dorsal margin about 0.8 length of ventral margin; valvura straight and slender.

Coloration (Figs 6F, 15): head yellowish brown, except vertex, ocellar area, frons, and dorsal portion of occiput brown; mesosoma yellowish brown, except mesoscutum, scutellum and dorsal surface of propodeum brown, speculum of mesopleuron yellowish white; wings hyaline, with wing vein and pterostigma yellowish brown; legs yellowish brown; metasoma yellowish brown.

Female (Fig. 16). General color and structure similar to male. HW/HL = 1.8–2.3 (1.92 ± 0.19); OD = 0.1–0.2 (0.16 ± 0.02) mm, POL/OD = 0.5–0.9 (0.67 ± 0.13); FW/FH = 1.0–1.2 (1.12 ± 0.07); CLW/CLH = 1.7–2.0 (1.80 ± 0.14); MSL/BMW = 0.4–0.5 (0.45 ± 0.06); GOI = 0.9–1.7 (1.24 ± 0.29); flagellum with 36–38 segments, 1st flagellomere 1.2–1.4 (1.32 ± 0.10) × as long as 2nd flagellomere, 3.9–5.9 (4.65 ± 0.80) × as long as wide. MSSL/MSSW = 1.1–1.3 (1.21 ± 0.08); SCL/SCW = 1.3–1.9 (1.48 ± 0.20); fore wing length 7.7–8.8 (8.37 ± 0.40) mm; RMI = 0.7–0.9 (0.78 ± 0.10); BNI = 0.1 (0.10 ± 0.04); hind wing with 5 hamuli; NI = 0.2–0.3 (0.26 ± 0.04). Fore tibial spur 0.3–0.4 (0.38 ± 0.03) × as long as 1st tarsomere; fore 1st tarsomere 9.6–15.4 (12.13 ± 1.92) × as long as wide, 1.7–2.2 (1.9 ± 0.18) × as long as 2nd; fore tarsal claw with 7–8 pectens; hind 1st tarsomere 10.0–14.2 (12.05 ± 1.73) × as long as wide, 2.0–2.1 (2.09 ± 0.04) × as long as 2nd; hind tarsal claw with 7–8 pectens. T1 3.7–4.4 (4.01 ± 0.26) × as long as posterior width, 1.4–1.8 (1.69 ± 0.16) × as long as T2; ovipositor 2.0–2.4 (2.19 ± 0.11) × as long as apical depth of metasoma.

Etymology. The specific name is derived from the type locality, Lake Dalupalringi, a pristine high-mountain lake located at the boundary between Kaohsiung City and Taitung County in Taiwan. This lake is famous for its difficulty to access and a sacred site for the indigenous Rukai people in Taiwan. The name is a noun in apposition.

Distribution. Taiwan (Kaohsiung, Nantou, Hualien).

Bionomics. Unknown.

Remarks. Given the differences mentioned above in the diagnosis section, especially the presence of the submarginal spine in the gonostyle and the pale body coloration, this species is considered a new species rather than a variant of *N.* (*Paro.*) *caucasica* (Kokujev, 1899). This species cannot be assigned into any known species group of this subgenus.

Discussion

The visibility of the pad after maceration may be influenced not only by the dissection protocol but also by its size and degree of sclerotization. Therefore, it is necessary to adjust the observation method according to the condition of each specimen. However, the lack of detailed explanations of observation techniques in the literature may increase the risk of character misinterpretation due to the use of inappropriate methods. As a mega-diverse genus with faunas in most biogeographic regions still requiring revision, we believe that the technique proposed herein will facilitate the systematic study of *Netelia* by providing standardized guidelines and reducing the possibility of character misinterpretation.

In previous morphological phylogenetic hypothesis of the genus *Netelia* proposed by Coronado-Rivera (2009), the subgenus *Paropheltes* was not recovered as a monophyletic group but polyphyletic in either analyses with or without successive weighting. This result may be at least partly attributed to the highly heterogeneous male genitalia within the group, as male genital characters are critical for the infrageneric classification of *Netelia*. In addition, some non-genital characters such as the state of the occipital carina and the location of fore wing vein 1cu-a relative to M&RS are also variable within the subgenus. The current *COI*-based phylogeny also recovered this subgenus as polyphyletic (Fig. 5B). Although *COI* alone may not provide sufficient resolution at higher phylogenetic nodes due to its highly divergent nature and potential biases introduced by genetic saturation, the current evidence, comprising the phylogenetic hypotheses and the ambiguous subgeneric boundaries between *Paropheltes* and *Longiterebates*, suggests that the current classification is artificial that underscores the need for future reclassification based on more comprehensive taxon and data sampling.

The described species of the subgenus *Paropheltes* are primarily distributed in the Palearctic (26 species) and Nearctic (11 species), accounting for 75% (36/48) of its known species richness (Yu et al. 2016). This distribution pattern suggests that the subgenus has a Holarctic center of biodiversity. The six species described from the Oriental region are primarily found in high-elevation areas of India and the Tibetan Plateau. A similar altitudinal distribution pattern is observed in Taiwanese species, which are found in mountainous regions above 1,300 m. For temperate-distributed taxa, it is common to inhabit higher elevations in tropical or subtropical regions (e.g., *Pseudalomya* (Chen et al. 2024), Ctenopelmatiae (Reshchikov 2015; Chen et al. 2025), and Ophioninae (Gauld and Mitchell 1981; Shimizu et al. 2016; Shimizu 2016, 2020). The discovery of this temperate subgenus in Taiwan highlights the underestimated species diversity shaped by the island's diverse habitats and remarkable elevation range.

Acknowledgements

We would like to express our sincere thanks to Chi-Feng Lee (TARI), Jing-Fu Tsai and Bao-Cheng Lai (NMNS), Kyohei Watanabe (KPMNH), Junsuke Yamasako, So Shimizu, and Yukinobu Nakatani (NARO), Masahiro Ohara and Juriya Okayasu (SEHU) for their kind supports during the specimen examinations of the first author and helping loaning the specimens; Oleksandr Varga (SIZU) for the photographs of the type specimens of *Netelia* (*Paropheltes*) *ermolenkoi* and *N.* (*Paro.*) *savchenkoi*; Chia-Lung Huang, Li-Hao Wang, Kuang-Yao Chen, Chien-Yu Huang, Yi Yang, and I-Lung Lee for the specimens; Kuan-Yao Chen and Yu-Feng Hsu for the collecting supports and permission of Taroko National Park, Hualien, Taiwan. We also thank Formosan Wild Sound Conservation Science Center Co., Ltd. (Miaoli, Taiwan) for providing the specimens collecting during their project "Ecological Fundamental Survey for Surrounding Environment of Dalupalringi Important Wetland and Kuaigu Lodge (111R51)"; the headquarter and Pingtung branch of Forestry and Nature Conservation Ageny, Ministry of Agriculture (Taiwan), the local tribes in Pingtung (Labwa, O'ponoho, Karamemedisane), and Vedai Township Office for the permission of the expedition; Lavakaw Dingiruru, Kecelre, Chen-Wei Ke, Wei-Hao Mai, Ren-Ming Syu, Bo-Cin Bao, Ljavakaw, and Syue-Cheng Wei for the supports during the expedition; Taiwan Entomological Society for funding the first authors' specimen investigation to KPMNH, NARO, and SEHU; International Society of Hymenopterists for the supports on the Article Processing Charges and grants for the first author. We also thank two reviewers for their valuable and constructive comments that improved the quality of the manuscript.

This study was funded by Taiwan's National Science and Technology Council [grant to the corresponding author: 111-2621-B-002-002], Ministry of Science and Technology (MOST) (current National Science and Technology Council) [grant to the first author: 109-2813-C-002-075-B], and Animal and Plant Health Inspection Agency, Ministry of Agriculture [grants to the corresponding author: 111AS-5.3.3-BQ-B2(2), 112AS-5.3.3-BQ-B2(2), and 112-RA-BQ-01(Z)].

This study is a part of the master's thesis of the first author (Chen 2024).

References

Altschul SF, Gish W, Miller W, Myers EW, Lipman DJ (1990) Basic local alignment search tool. Journal of Molecular Biology 215: 403–410. https://doi.org/10.1016/S0022-2836(05)80360-2

Andersson H (1972) En snabb och billig metod att montera genitalpreparat i glycerin. Entomologen 1: 1–2.

Aubert JF, Halperin J, Gerling D (1984) Les ichneumonides d'israel. Entomophaga 29: 211–235. https://doi.org/10.1007/BF02372110

Bennett AMR (2015) Revision of the world genera of Tryphoninae (Hymenoptera: Ichneumonidae). Memoirs of the American Entomological Institute 86: 1–387.

Bennett AMR, Cardinal S, Gauld ID, Wahl DB (2019) Phylogeny of the subfamilies of Ichneumonidae (Hymenoptera). Journal of Hymenoptera Research 71: 1–156. https://doi.org/10.3897/jhr.71.32375

Brischke CGA (1880) Die Ichneumoniden der Provinzen West- und Ost-Preussen. Schriften der Naturforschenden Gesellschaft in Danzig 4(4): 108–210.

Broad GR, Shaw MR, Fitton MG (2018) Ichneumonid Wasps (Hymenoptera: Ichneumonidae): their classification and biology. Handbooks for the identification of the British insects 7(12): 1–418. https://doi.org/10.1079/9781800625471.0000

Cameron P (1907) Description of a new genus and some new species of Hymenoptera captured by Lieut.-Col. C.G. Nurse at Deesa, Matheran and Ferozepore. Journal of the Bombay Natural History Society 17: 1001–1012.

Chen H-P (2024) Systematics of the genus *Netelia* Gray, 1860 (Hymenoptera, Ichneumonidae, Tryphoninae) of Taiwan—A focus on the non-nominotypical subgenera. Master thesis, National Taiwan University, Taipei, 485 pp. https://doi.org/10.6342/NTU202402092

Chen H-P, Huang C-L, Shiao S-F (2025) A taxonomic revision of the genus *Alexeter* Förster (Hymenoptera, Ichneumonidae, Ctenopelmatinae, Mesoleiini) from Taiwan, with descriptions of six new species. ZooKeys 1250: 315–358. https://doi.org/10.3897/zookeys.1250.156835

Chen H-P, Kikuchi N, Shiao S-F (2024) Discovery of a new *Pseudalomya* Telenga, 1930 (Hymenoptera, Ichneumonidae, Ichneumoninae) species from Taiwan and its implications for the systematic position of this genus. Journal of Hymenoptera Research 97: 277–296. https://doi.org/10.3897/jhr.97.119470

Chen H-P, Lin K-T, Wu S (2023) Re-evaluation of the taxonomic confusion of the metallic-blue *Pimpla* Fabricius, 1804 (Hymenoptera: Ichneumonidae: Pimplinae) species in the Oriental region. Zootaxa 5357(2): 270–284. https://doi.org/10.11646/zootaxa.5357.2.5

Chiu S, Chou L, Chou K (1984) A check list of Ichneumonidae (Hymenoptera) of Taiwan. Special Publication of The Taiwan Agricultural Research Institute 15: 1–67.

Choi JK, Lee JW (2017) Taxonomy of the subgenus *Parabates* Förster of *Netelia* Gray, 1860 (Hymenoptera: Ichneumonidae: Tryphoninae) from South Korea. Korean Journal of Applied Entomology 56(3): 283–287. https://doi.org/10.5656/KSAE.2017.06.0.009

Choi JK, Lee JW (2019) A taxonomic review of the North Korean *Netelia* Gray, 1860 (Hymenoptera: Ichneumonidae: Tryphoninae). Journal of National Park Research 10(1): 182–196.

Coronado-Rivera J (2009) Filogenia de avispas del género *Netelia* (Hymenoptera: Ichneumonidae) con énfasis en las especies costarricenses. Revista de Biología Tropical 57: 213–238. https://doi.org/10.15517/rbt.v57i0.32903

Cruaud A, Nidelet S, Arnal P, Weber A, Fusu L, Gumovsky A, Huber J, Polaszek A, Rasplus J-Y (2019) Optimized DNA extraction and library preparation for minute arthropods: Application to target enrichment in chalcid wasps used for biocontrol. Molecular Ecology Resources 19: 702–710. https://doi.org/10.1111/1755-0998.13006

Dal Pos D, Mikó I, Talamas EJ, Vilhelmsen L, Sharanowski BJ (2023) A revised terminology for male genitalia in Hymenoptera (Insecta), with a special emphasis on Ichneumonoidea. Peer J 11: e15874. https://doi.org/10.7717/peerj.15874

Dayrat B (2005) Towards integrative taxonomy. Biological Journal of the Linnean Society 85: 407–415. https://doi.org/10.1111/j.1095-8312.2005.00503.x

Delrio G (1975) Révision des espèces ouest-paléarctiques du genre *Netelia* Gray (Hym., Ichneumonidae). Studi Sassaresi Sez.III.-Annali della Facolta di Agraria dell'Università di Sassari 23: 1–126.

Eady RD (1968) Some illustrations of microsculpture in the Hymenoptera. Proceedings of the Royal Entomological Society of London 43: 66–72. https://doi.org/10.1111/j.1365-3032.1968.tb01029.x

Folmer O, Black M, Hoeh W, Lutz R, Vrijenhoek R (1994) DNA primers for amplification of mitochondrial cytochrome c oxidase subunit I from diverse metazoan invertebrates. Molecular Marine Biology and Biotechnology 3(5): 294–299.

Gauld ID (1997) Ichneumonidae of Costa Rica, 2. Memoirs of The American Entomological Institute 57: 1–485.

Gauld ID, Mitchell PA (1981) The taxonomy, distribution and host preferences of Indo-Papuan parasitic wasps of the subfamily Ophioninae. CAB Slough / Commonwealth Institute of Entomology, London, 611 pp.

Gray JE (1860) On the hook on the front edge of the hind wing of certain Hymenoptera. Annals and Magazine of Natural History 3(5): 339–342. https://doi.org/10.1080/00222936008697226

Guindon S, Dufayard J-F, Lefort V, Anisimova M, Hordijk W, Gascuel O (2010) New Algorithms and Methods to Estimate Maximum-Likelihood Phylogenies: Assessing the Performance of PhyML 3.0. Systematic Biology 59(3): 307–321. https://doi.org/10.1093/sysbio/syq010

Hajibabaei M, Janzen DH, Burns JM, Hallwachs W, Hebert PDN (2006) DNA barcodes distinguish species of tropical Lepidoptera. Proceedings of the National Academy of Sciences 103: 968–971. https://doi.org/10.1073/pnas.0510466103

He J, Gao Z, Su Y, Lin S, Jiang H (2018) Geographical and temporal origins of terrestrial vertebrates endemic to Taiwan. Journal of Biogeography 45: 2458–2470. https://doi.org/10.1111/jbi.13438

Hebert PDN, Cywinska A, Ball SL, Dewaard JR (2003a) Biological identifications through DNA barcodes. Proceedings of the Royal Society B 270: 313–321. https://doi.org/10.1098/rspb.2002.2218

Hebert PDN, Ratnasingham S, de Waard JR (2003b) Barcoding animal life: cytochrome c oxidase subunit 1 divergences among closely related species. Proceedings of the Royal Society of London B: Biological Sciences 270: S96–S99. https://doi.org/10.1098/rsbl.2003.0025

Hebert PDN, Penton EH, Burns JM, Janzen DH, Hallwachs W (2004) Ten species in one: DNA barcoding reveals cryptic species in the neotropical skipper butterfly *Astraptes fulgerator*. Proceedings of the National Academy of Sciences 101: 14812–14817. https://doi.org/10.1073/pnas.0406166101

Hoang DT, Chernomor O, von Haeseler A, Minh BQ, Vinh LS (2017) UFboot2: Improving the Ultrafast Bootstrap Approximation. Molecular Biology and Evolution 35(2): 518–522. https://doi.org/10.1093/molbev/msx281

Kalyaanamoorthy S, Minh BQ, Wong TKF, von Haeseler A, Jermiin LS (2017) Modelfinder: Fast model selection for accurate phylogenetic estimates. Nature Methods 14: 587–589. https://doi.org/10.1038/nmeth.4285

Katoh K, Rozewicki J, Yamada KD (2019) MAFFT online service: Multiple sequence alignment, interactive sequence choice and visualization. Briefings in Bioinformatics 20(4): 1160–1166. https://doi.org/10.1093/bib/bbx108

Kaur R, Jonathan JK (1976) A new Tryphonine subgenus *Longiterebates* from India (Hymenoptera: Ichneumonidae). Oriental Insects 10(1): 33–37. https://doi.org/10.1080/00305316.1976.10432319

Kaur R, Jonathan JK (1979) Ichneumonologica Orientalis, Part VIII. The tribe Phytodietini from India (Hymenoptera: Ichneumonidae). Oriental Insects Monograph 9: 1–276.

Klose C (2006) Climate and geomorphology in the uppermost geomorphic belts of the Central Mountain Range, Taiwan. Quaternary International 147(1): 89–102. https://doi.org/10.1016/j.quaint.2005.09.010

Konishi K (1985) A revison of the subgenus *Parabates* Foerster of the genus *Netelia* Gray from Japan (Hymenoptera, Ichneumonidae). Kontyû 53(4): 616–624.

Konishi K (1986a) A revision of the subgenus *Apatagium* Enderlein of the genus *Netelia* Gray from Japan (Hymenoptera, Ichneumonidae). Kontyû 54(2): 261–270.

Konishi K (1986b) A new subgenus and species of the genus *Netelia* (Hymenoptera, Ichneumonidae) from New Guinea. Kontyû 54(3): 415–419.

Konishi K (1991) A revision of the subgenus *Prosthodocis* Enderlein of the genus *Netelia* Gray of Japan (Hymenoptera, Ichneumonidae), I. Kontyû 59(4): 775–788.

Konishi K (1992) A revision of the subgenus *Prosthodocis* Enderlein of the genus *Netelia* Gray of Japan (Hymenoptera, Ichneumonidae), II. Kontyû 60(1): 39–53.

Konishi K (1996a) A revision of the subgenus *Paropheltes* Cameron of the genus *Netelia* GRAY (Hymenoptera, Ichneumonidae) of Japan. Japanese Journal of Entomology 64(1): 163–187.

Konishi K (1996b) A new species of the subgenus *Apatagium* Enderlein of the genus *Netelia* GRAY from Japan (Hymenoptera, Ichneumonidae). Japanese Journal of Entomology 64(2): 236–240.

Konishi K (1996c) Study on the subgenus *Toxochiloides* Tolkanitz of the genus *Netelia* GRAY (Hymenoptera, Ichneumonidae) of Japan. Japanese Journal of Entomology 64(3): 473–481.

Konishi K (2000) Distributional and nomenclatural notes on some species of *Netelia* (Hymenoptera: Ichneumonidae). Zoosystematica rossica 8(2): 290.

Konishi K (2005) A preliminary revision of the subgenus *Netelia* of the genus *Netelia* from Japan (Hymenoptera, Ichneumonidae, Tryphoninae). Insecta Matsumurana New Series 62: 45–121.

Konishi K (2010) Taxonomic status of *Amebachia* Uchida in the genus *Netelia* Gray (Hymenoptera; Ichneumonidae; Tryphoninae) with descriptions of four new species from Japan. Entomological Science 13: 216–225. https://doi:10.1111/j.1479-8298.2010.00376.x

Konishi K (2012) A new species of the subgenus *Protonetelia* of the genus *Netelia* from Taiwan (Hymenoptera, Ichneumonidae, Tryphoninae). Esakia 52: 67–70. https://doi.org/10.5109/25398

Konishi K (2014) A revision of the subgenus *Bessobates* of the genus *Netelia* from Japan (Hymenoptera, Ichneumonidae, Tryphoninae). Zootaxa 3755(4): 301–346. https://doi.org/10.11646/zootaxa.3755.4.1

Konishi K, Chen H-P, Pham NT (2022) A taxonomic review of the genus *Netelia*, subgenus *Monomacrodon* (Hymenoptera: Ichneumonidae: Tryphoninae), with description of a new species. The Raffles Bulletin of Zoology 70: 376–384. https://doi.org/10.26107/RBZ-2022-0019

Lee JW, Cha JY (1996) Taxonomy and phylogeny of the subfamily Tryphoninae (Hymenoptera: Ichneumonidae) IV. A review of tribe Phytodietini. Entomological Research Bulletin (KEI) 22: 35–49.

Minh BQ, Schmidt HA, Chernomor O, Schrempf D, Woodhams MD, von Haeseler A, Lanfear R (2020) IQ-TREE 2: New Models and Efficient Methods for Phylogenetic Inference in the Genomic Era. Molecular Biology and Evolution 37(5): 1530–1534. https://doi.org/10.1093/molbev/msaa015

Morley C (1915) Ichneumonologia Britannica. Vol. 5. Ichneumons of Great Britain. Ophioninae. H. and W. Brown, London, 400 pp.

Pham NT, Chen H-P, Konishi K (2021) Notes on the genus *Netelia*, subgenus *Parabates* (Ichneumonidae, Tryphoninae), with description of a new species from Oriental Region. Zootaxa 4974(3): 577–584. https://doi.org/10.11646/zootaxa.4974.3.6

Puillandre N, Brouillet S, Achaz G (2020) ASAP: assemble species by automatic partitioning. Molecular Ecology Resources 21(2): 609–620. https://doi.org/10.1111/1755-0998.13281

Ratnasingham S, Hebert PDN (2007) BOLD: The Barcode of Life Data System (http://www.barcodinglife.org). Molecular Ecology Notes 7: 355–364. https://doi.org/10.1111/j.1471-8286.2007.01678.x

Reshchikov A (2015) The World Fauna of the Genus *Lathrolestes* (Hymenoptera, Ichneumonidae). PhD Thesis, University of Tartu, Tartu, 246 pp.

Shimizu S (2016) Distributional notes on *Leptophion giganteus* Shimizu & Watanabe, 2016 (Hymenoptera: Ichneumonidae: Ophioninae). Japanese Journal of Systematic Entomology 22: 199–201.

Shimizu S (2020) The Nepalese species of the genus *Enicospilus* Stephens, 1835 (Hymenoptera, Ichneumonidae, Ophioninae): a preliminary revision and identification key to species. Deutsche Entomologische Zeitschrift 67: 69–126. https://doi.org/10.3897/dez.67.51332

Shimizu S, Watanabe K, Maeto K (2016) Revision of the Taiwanese species of the genus *Leptophion* Cameron, 1901 (Hymenoptera: Ichneumonidae: Ophioninae), with a discussion of their phenology and distribution. Zootaxa 4144: 71–88. https://doi.org/10.11646/zootaxa.4144.1.3

Shimizu S, Broad GR (2020) Photographic catalogue of the oldest primary types of Japanese Ichneumonoidea (Hymenoptera), those described by Frederick Smith and Francis Walker in 1874. Journal of Natural History 54(17–18): 1115–1198. https://doi.org/10.1080/00222933.2020.1776905

Tamura K, Stecher G, Kumar S (2021) MEGA11: Molecular Evolutionary Genetics Analysis Version 11. Molecular Biology and Evolution 38(7): 3022–3027. https://doi.org/10.1093/molbev/msab120

Tolkanitz VI (1974) Revision of the genus *Netelia* (Hymenoptera, Ichneumonidae) and review of species of the fauna of the USSR. Zoologicheskii Zhurnal 53: 376–393.

Tolkanitz VI (1981a) Fauna Ukraini. [Vol. 11. Parasitic Hymenoptera. Part 1. Ichneumonidae - Phytodietini.] Akademia Nauk Ukrainskoi SSR (Kiev), 148 pp.

Tolkanitz VI (1981b) Ichneumonid genus *Netelia* (Hymenoptera, Ichneumonidae) of Far East. In: Ler PA, Kupyanskaya AN, Lelej AS, Fedikova VS (Eds) Hymenoptera of the Far East. (Vladovostok), 26–40.

Tolkanitz VI (1999) New data on the fauna of the genus *Netelia* (Hymenoptera, Ichneumonidae) of the Russian Far East. Zoologicheskii Zhurnal 78: 633–634.

Townes HK (1939) The Nearctic species of *Netelia* (*Paniscus* of authors) and a revision of genera of Neteliini (Hymenoptera, Ichneumonidae). Lloydia 1: 168–231.

Townes HK, Townes M, Gupta VK (1961) A catalogue and reclassification of the Indo-Australian Ichneumonidae. Memoirs of the American Entomological Institute 1: 1–522.

Uchida T (1928) Zweiter Beitrag zur Ichneumoniden-Fauna Japans. Journal of the Faculty of Agriculture, Hokkaido Imperial University 21: 177–297.

Uchida T (1934) Beitrage zur Systematik der Tribus Paniscini Japans (Hym., Ichneum. Tryphoninae). Insecta Matsumurana 8: 107–115.

Yeates DK, Seago A, Nelson L, Cameron SL, Joseph LEO, Trueman JW (2011) Integrative taxonomy, or iterative taxonomy? Systematic entomology 36(2): 209–217. https://doi.org/10.1111/j.1365-3113.2010.00558.x

Yu DSK, van Achterberg C, Horstmann K (2016) Taxapad 2016, Ichneumonoidea 2015. Ottawa, Ontario. http://www.taxapad.com [database on flash-drive]

Zhang J, Kapli P, Pavlidis P, Stamatakis A (2013) A general species delimitation method with applications to phylogenetic placements. Bioinformatics 29(22): 2869–2876. https://doi.org/10.1093/bioinformatics/btt499

Supplementary material 1

Information of the specimens and sequences used in this study

Author: Hsaun-Pu Chen

Data type: xlsx

Explanation note: Detailed information of the specimens and sequences used in this study.

Copyright notice: This dataset is made available under the Open Database License (http://opendatacommons.org/licenses/odbl/1.0/). The Open Database License (ODbL) is a license agreement intended to allow users to freely share, modify, and use this Dataset while maintaining this same freedom for others, provided that the original source and author(s) are credited.

Link: https://doi.org/10.3897/jhr.99.167713.suppl1

Supplementary material 2

Files for molecular phylogeny and species delimitation analyses.
Author: Hsaun-Pu Chen
Data type: zip
Explanation note: Fasta, nexus, and treefile files for the analyses in this study.
Copyright notice: This dataset is made available under the Open Database License (http://opendatacommons.org/licenses/odbl/1.0/). The Open Database License (ODbL) is a license agreement intended to allow users to freely share, modify, and use this Dataset while maintaining this same freedom for others, provided that the original source and author(s) are credited.
Link: https://doi.org/10.3897/jhr.99.167713.suppl2

Supplementary material 3

The measurements, ratios, and meristic counts
Author: Hsaun-Pu Chen
Data type: pdf
Explanation note: This file summarized the measurements, ratios, and meristic counts of the Taiwanese species of subgenus *Parapheltes*, genus *Netelia*.
Copyright notice: This dataset is made available under the Open Database License (http://opendatacommons.org/licenses/odbl/1.0/). The Open Database License (ODbL) is a license agreement intended to allow users to freely share, modify, and use this Dataset while maintaining this same freedom for others, provided that the original source and author(s) are credited.
Link: https://doi.org/10.3897/jhr.99.167713.suppl3

Supplementary material 4

The original photos of the male genitalia
Author: Hsaun-Pu Chen
Data type: pdf
Explanation note: The original photos of the male genitalia for the species described in this studye.
Copyright notice: This dataset is made available under the Open Database License (http://opendatacommons.org/licenses/odbl/1.0/). The Open Database License (ODbL) is a license agreement intended to allow users to freely share, modify, and use this Dataset while maintaining this same freedom for others, provided that the original source and author(s) are credited.
Link: https://doi.org/10.3897/jhr.99.167713.suppl4